Airflow and hail growth in supercell storms and some implications for hail suppression

by

K. A. Browning[1] and G. B. Foote[2]
National Center for Atmospheric Research
Boulder, Colorado

[1]On leave from the Meteorological Office Research Unit, Royal Radar Establishment, Malvern, England.

[2]This research was performed as part of the National Hail Research Experiment, managed by the National Center for Atmospheric Research and sponsored by the Weather Modification Program, Research Applications Directorate, National Science Foundation.

ABSTRACT

Multiple radar and aircraft observations of a damaging supercell hailstorm in northeastern Colorado are synthesized to show that the airflow and hail growth conformed in many respects to earlier models derived by the lead author. Some features that before had to be inferred indirectly are now substantiated and elaborated upon by direct observation. As a result of our increased confidence in certain aspects of the model we have been able to draw implications regarding the feasibility of suppressing hail by different means.

The observations indicate that an important stage in the growth of large hail is the entry of hailstone embryos into the edge of an intense updraft. These embryos are grown near the storm's right flank and get carried around the forward flank under the influence of a strong environmental airstream which divides at the stagnation point and flows around on either side of the main updraft. The main updraft itself is characterized by a weak-echo vault and the embryos grow into large hail as they follow a simple up-and-down trajectory over it.

The vault takes on added significance in that it is a symptom of inefficiency in the conversion of cloud water to precipitation. Paradoxically it is this very inefficiency that encourages the growth of large hail by minimizing the effects of competition for the available supercooled droplets. Those recirculating embryos that find their way to the edge of the vault via the embryo curtain are seen to compete unfairly by being the first to encounter the undepleted cloud water in the vault. It is difficult to suppress their growth artificially because seeding in the main updraft at economical rates produces particles that rise above the hail growth region before they can have any significant influence on the available water.

The existence of a large vault implies that the flow field is so restricting the number of embryos re-entering the main updraft that they may be sweeping up only a small proportion of the overall cloud water. Thus there is a danger that, if a mode of seeding were used which caused additional embryos to re-enter the updraft along with the re-entering natural embryos, this would lead to the production of additional large hailstones. Hence, at least for some storms, doubt is cast on the credibility of the competing embryo hypothesis for hail suppression, according to which the generation of additional embryos by seeding is supposed to promote competition for a restricted amount of cloud water to the extent that none can grow large.

---

1. Introduction

Experiments to suppress hail using silver iodide seeding have been conducted in many countries during the last decade. Conclusions drawn from these experiments differ greatly and there is still no consensus about the effectiveness of seeding as a means of suppressing hail. This is hardly surprising since our ignorance of the manner in which hail grows in natural clouds constrains one to seek statistical evaluations of seeding experiments conducted on the basis of unverified hypotheses. So great is the temporal and point-to-point variability of natural hailfalls and so infrequent is the incidence of hail, that it seems difficult to obtain statistically convincing results from experimental programs of this kind unless the programs are continued for unacceptably long periods (Hitschfeld, 1974).

Most suppression efforts are based upon the idea that the growth of hailstones can be inhibited by creating more embryos which will compete for the available water to the extent that none grows large. Undoubtedly seeding generates more potential embryos. However, there is no assurance that the seeding is able to produce sufficient embryos in the right place to be able to compete effectively. Neither can there be any such assurance until it is known where the natural embryos are produced and where and how they grow into hailstones. It is possible, for example, that abundant embryos are generated naturally but that the storm circulation exerts a natural selection mechanism that tends to prevent large concentrations of embryos from entering and lingering in the regions of the updraft where hailgrowth can occur (Ludlam, 1964). Hence, it is important to know more about the growth history and trajectories of natural precipitation particles in order to find out where, if at all, one should attempt to stimulate the growth of further embryos.

Only by obtaining a better physical understanding of the growth of natural hail will it become possible to adjust seeding techniques to the requirements of the situation and to design appropriate physical evaluations of the effects of such seeding. Even if partial success in a particular method of suppressing hail were demonstrated statistically, without such understanding we would still not know how to improve existing seeding techniques or how to adapt them to other kinds of storms. Thus one of the goals of the National Hail Research Experiment (NHRE) is to develop observationally-based kinematic models of the airflow and precipitation trajectories within different classes of hailstorms. This paper is a step in that direction. We shall present the results of a case study on the basis of which we derive a model representative of a particular kind of hailstorm known as a supercell storm. The model resembles earlier models derived by the lead author; however, the quality of data in the present study is such that the model is refined to the stage that detailed implications can be drawn regarding the growth of hail and possible ways of suppressing it.

The essence of this study is the synthesis of data from several sources but, even with data from an elaborate observational program of the kind mounted by NHRE, a certain amount of speculation is still needed to reconstruct a useful picture of the overall hailstorm organization. While future NHRE field programs will no doubt make observations that are more definitive, the present requirement for a synthesized flow field is so crucial that we believe a limited amount of speculation can be tolerated so long as it is based upon sound physical reasoning.

2. The supercell storm as a distinct hailstorm category

Several categories of hailstorms have been proposed, such as squall line storms, multicell storms, supercell storms and severely sheared storms (Marwitz,

1972, a, b, c; Chisholm, 1973). Of these categories perhaps two of the most basic are the multicell and supercell storms (Chisholm and Renick, 1972). Most hailstorms fall into the multicell category and consist of sequences of cells each of which goes through the familiar updraft-downdraft life cycle described by Byers and Braham (1949). However, a few hailstorms are characterized by a single persistent cell which generally travels appreciably to the right* of the winds (in the Northern Hemisphere) while retaining a quasi-steady structure, with updraft and downdraft coexisting symbiotically for periods long compared with the time taken for air to pass through the storm. These are the supercell storms, and although they constitute a small proportion of all hailstorms, they probably cause a disproportionate amount of damage (Summers, 1972) owing to the large hail size and the duration and extent of the hail they produce.

The name supercell was first used (Browning, 1962) to describe the quasi-steady state structure attained by the Wokingham hailstorm during its intense phase. Similar radar structures were subsequently identified in severe hailstorms in Oklahoma (Browning and Donaldson, 1963; Browning, 1965a). An important feature of the radar echo from each of these storms was a distinctively shaped region devoid of detectable echo which penetrated upward into the core of the storm beneath its highest top. Browning and Ludlam (1962) called this the echo-free vault. The vault was considered to be an important feature since it identified the location of an updraft so strong that not only did large hydrometeors not have time to form within it, but also hydrometeors formed elsewhere were prevented from falling back into a large part of it. These inferences are well known but

* Occasionally left

they are thought to have far-reaching consequences for hail growth and hail suppression, which we shall be investigating further in this paper.

Recent studies using radars of improved resolution have shown that a weak-echo region (WER) can be found in most hailstorms whether they are multicell or supercell (Marwitz, 1972a,b; Chisholm, 1973). Aircraft penetrations and radar-tracked chaff have confirmed that the WER's are indeed regions of updraft (Marwitz and Berry, 1971; Marwitz, 1973a). It has also become evident that not all storms fitting the supercell definition have the archetypal vault structure (also referred to as a bounded weak-echo region by Chisholm (1970), because at some altitude the vault is bounded on all sides by echo). Many supercells, and probably most multicell storms have merely an unbounded weak-echo region (e.g., Chisholm, 1973); that is, a WER surmounted by echo aloft but not bordered by echo on all sides. Whether bounded or unbounded, an important difference between the WER in multicell and supercell storms is its persistence. In the supercell case it may persist for periods on the order of an hour or more. In multicell storms the WER and other radar echo features tend to be rather transitory.

While the main characteristic of the supercell storm is the steadiness of the organized flow field, rather than very specific features of the radar structure, it appears that the most damaging hailfalls (and also tornadoes) are associated with the archetypal supercell described previously and illustrated in Fig. 1. It is such a storm that is the subject of the current paper. Storms of this type require a rather special set of environmental conditions, including strong instability in combination with strong vertical wind shear and usually strong vertical wind veer. As a result such supercells have a distinctive structure. Because of this it is possible to derive airflow models for these storms that have a more general applicability than would be the case, for example, for models

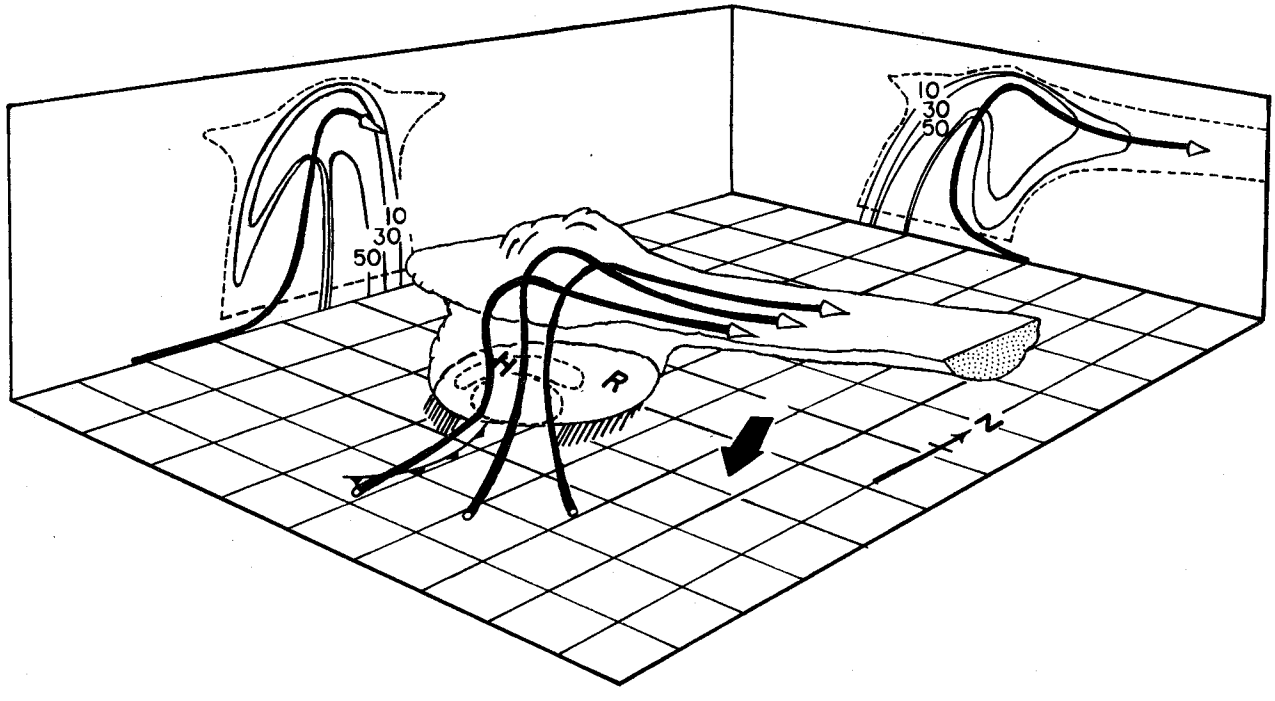

Fig. 1 Perspective view of a supercell storm showing mean streamlines and reflectivity structure (after Chisholm and Renick, 1972).

describing the more highly variable multicell storms which occur for a wider variety of environmental conditions.

In this paper we shall attach a great deal of importance to two features of the echo pattern shown in Fig. 1. One of these is the vault itself. The other is the curtain of echo bounding the southern edge of the vault at levels above about 4 km and situated over the inflow. This has been referred to previously as the forward overhang by Browning and Ludlam (1962) and the giant curved streamer by Browning (1965b). However, we shall call it the embryo curtain, because, as we shall show, parts of it are important as a source of hailstone embryos.

3. Nature of the data

Emphasis in this paper is on a generalized motion field deduced from a particular case study, but thought to be applicable to a class of supercell storms. The flow field is studied within the unifying context of the three-dimensional radar echo structure, and the combination of air motion and radar information is used to deduce plausible regions of hail formation and growth and to examine the feasibility of current hail suppression techniques.

The storm model developed here is based on the study of a damaging supercell which occurred on 21 June 1972 in the vicinity of the NHRE networks in northeastern Colorado. Giant hail was first reported at Fleming, Colo., and we shall henceforth call it the Fleming storm. The storm met the criteria for inclusion in the NHRE hail suppression experiment (outlined by Lovell, 1974) and was seeded at cloud base with silver iodide flares from 1430 to 1610 MDT as it skirted the northeastern corner of the target area. The seeding rate was about 60 g min^{-1}. No effects which could definitely be attributed to this seeding have been discerned, and we assume in this study that none of the important measurements was affected by the seeding.

Instrumented aircraft and conventional meteorological radars were the principal data sources for the present analysis. Four aircraft equipped to measure horizontal wind and the state parameters, along with other variables, flew around and under the storm. They were a DC-6 and a C-130 from the NOAA Research Flight Facility, and a Queen Air and Buffalo from NCAR's Research Aviation Facility. Flight patterns involved the Queen Air monitoring conditions at cloud base while the Buffalo and DC-6 flew circuits around the storm at two sub-cloud levels and the C-130 circumnavigated the storm in the mid-troposphere. The Queen Air and C-130 used Doppler navigation systems for computing winds. The Buffalo was equipped with an inertial system. The DC-6 wind-finding system was not operating properly, and winds from that aircraft were not reliable; other measurements were useful, however. All important aircraft measuring systems had been calibrated and intercompared at the start of the field season.

The radar systems included the high-resolution (1° beam) 10-cm radar at Grover, operated by NCAR personnel, a similar system known as the CHILL radar, located near Ft. Morgan and operated jointly by the University of Chicago and the Illinois State Water Survey, the WSR-57 radar of the National Weather Service located near Limon, Colorado, and the RDR-1 3-cm side-looking tail radar carried by the DC-6. This radar performed a helical scan about a horizontal axis as the aircraft moved forward. Although the RDR-1 had a 3° beam, at the close ranges involved (< 10 km) it provided the highest resolution of any of the radars mentioned. However, it suffered severely from attenuation problems and was not suitable for most quantitative purposes. The WSR-57 provided the most complete temporal coverage of the storm, but at the approximately 200 km range involved, it had poor resolution. The Grover radar provided quantitative digital data with a resolution of 1-2 km, and is given primary emphasis here. Photographs of a PPI

scope were the only data available from the CHILL radar. This radar provided good temporal coverage of the storm during all the important phases, and was useful in establishing the steadiness of the echo configuration after the storm moved out of range of the Grover radar.

Other useful observations include serial ascents at 90-min intervals from four NHRE rawinsonde sites, airborne and ground-based cloud photography, and surface reports of rain and hail which, along with crop insurance data, establish the extent of the hailswath and the typical hailstone size.

Particularly important in this study are the fast (1 min) scan sequences of the Grover radar, which enable one to track small reflectivity maxima through the storm and thus infer the internal air motion. This, along with the large (perhaps unprecedented) variety of other data on a single such storm, comprise the novel features here, and allow one to piece together an integrated picture of the general hail-forming mechanisms with more confidence than in previous studies.

4. General description of the storm

(a) The storm track and surface hail

Figure 2 shows the hourly positions of the Fleming storm as monitored by the Limon radar (positions at 1500 and earlier from the CHILL radar). The storm was first detected at 1245, as a cluster of small rain showers located about 30 km northeast of Cheyenne, Wyoming. The storm formed on the confluent leading edge of a tongue of low-level moisture moving from the south-southeast across northeastern Colorado, western Kansas and Nebraska. Conditions at Cheyenne were typical of the region on the west side of the confluence line, with dry westerly surface winds blowing off the mountains throughout the day. The upper-level winds revealed a generally zonal west-northwesterly flow, with the important

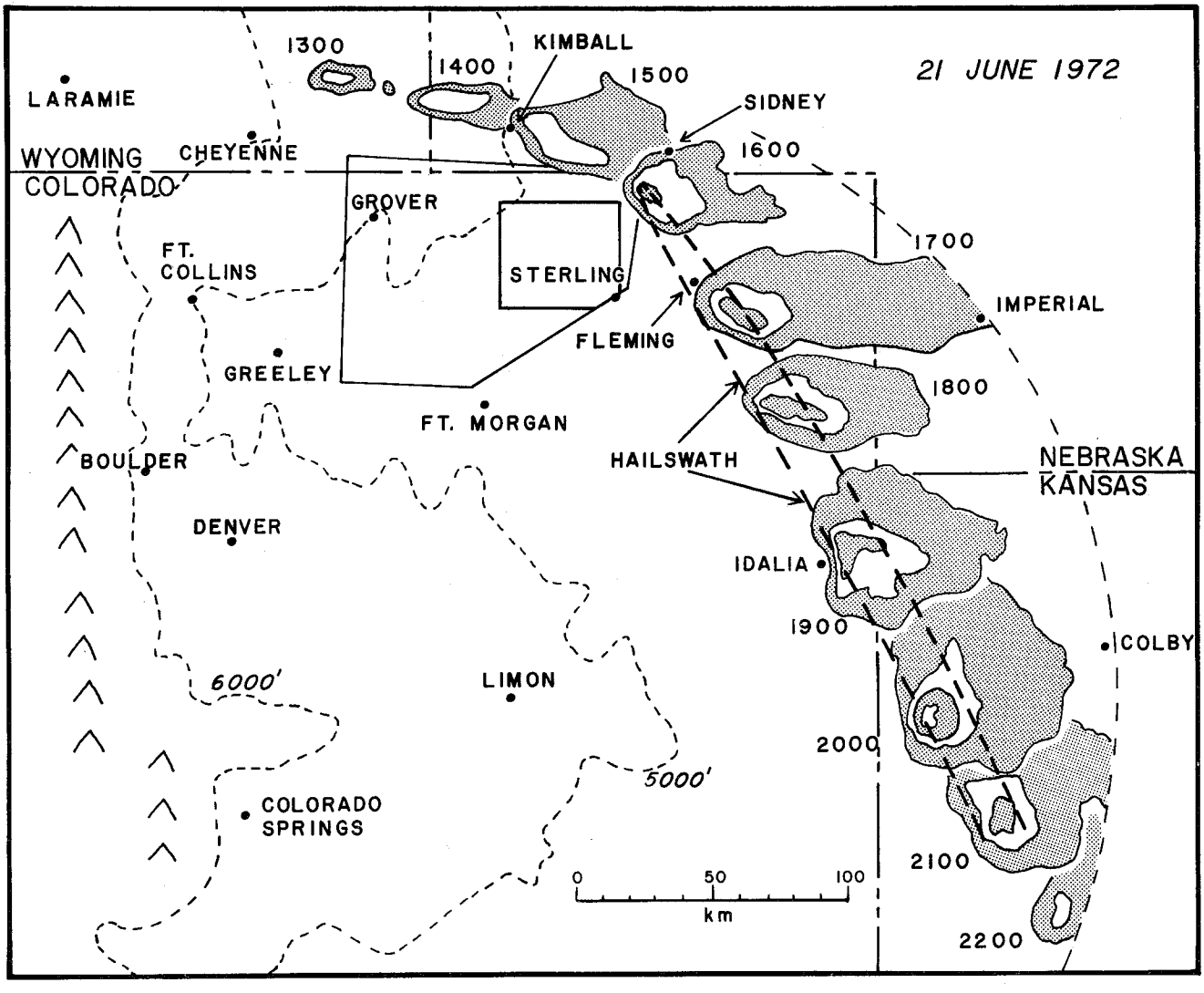

Fig. 2 Hourly positions of the Fleming hailstorm as determined by the NWS Limon radar (CHILL radar data used 1300-1500 MDT). The approximate limits of the hailswath are indicated by the bold dashed line. Continuity of the swath is not well established but total extent is. Special rawinsonde sites were located near the towns of Grover, Ft. Morgan, Sterling and Kimball. Contour intervals are roughly 12 dB above 20 dBZ.

synoptic feature being a jet core located from central Wyoming through southern Nebraska and into Kansas, thus placing the NHRE area in a region of significant divergence aloft.

The small initial echoes from the storm quickly consolidated and moved roughly in the direction of the mean cloud-layer winds into a region of higher surface moisture. The storm intensified and made an abrupt turn to the right near 1555, thereafter moving from 335°, some 50° to the right of the mean winds. The storm had an evolving multi-cellular structure until 1500-1530, when it started to take on supercell characteristics. By the time it turned to the right, radar analysis shows it had reached a quasi-steady configuration. Detailed analyses presented in later sections deal with the storm after the steady state was attained.

Although hail half-inch in diameter was reported near 1430 as the storm passed over the Kimball airport, it appears that the most damaging hail began near Peetz at the time the storm made its turn, with hailstones as big as golf balls being reported (at start of bold dashed curve in Fig. 2). Fig. 3 is a photograph looking southeastward taken at 1615, showing the heavy precipitation, part of the hailswath, and the western boundaries of the cloud. Hail the size of baseballs first fell near the town of Fleming at about 1700 (see Fig. 2 for locations) and was subsequently reported fairly consistently over a 30 km length of the swath, a distance traveled by the storm in about 40 min. It may have fallen over a substantially longer period in the life of the storm, but data are not available on this point. Reports from local residents and from insurance claims indicate that the hailswath was 15-20 km wide. Crop damage was severe and continued over a 200 km length of the swath, far into Kansas.

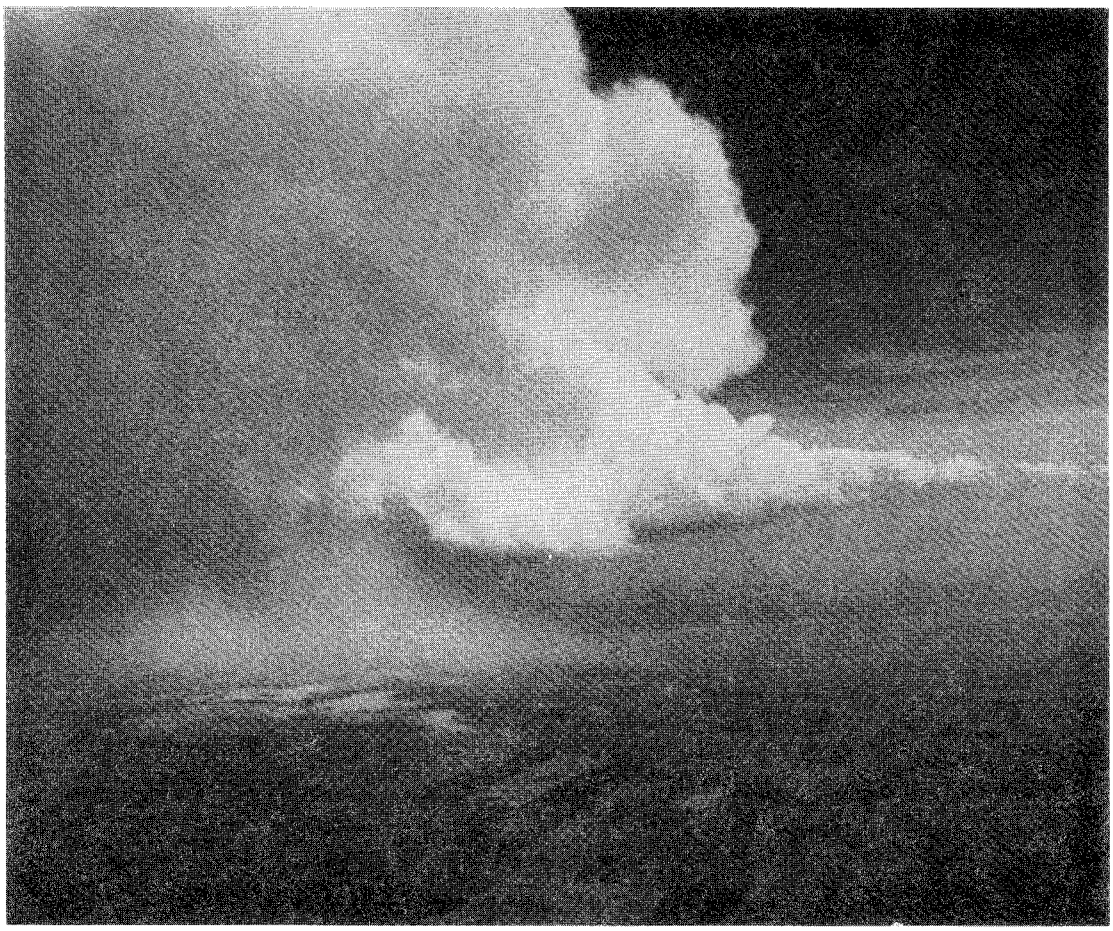

Fig. 3 Photograph looking southeast toward the western flank of the Fleming storm showing hailswath on ground and dense curtain of precipitation. Photograph taken 35 km from the storm.

It appears from the Limon radar data in Fig. 2 that the storm continued to intensify after the period of study emphasized here, approximately 1600 to 1700. This is consistent with its movement toward regions of higher surface dew point and hence greater instability. A tornado was reported from the storm near Idalia at 1840. The storm was dissipating as it moved out of radar range at 2200. The total lifetime was in excess of 9 hours, at least 5 of which were spent in the severe right-moving stage.

(b) Environmental soundings

Fig. 4 shows the hodograph for the 1541 sounding from Sterling, released about 50 km south of the storm's position then (see Fig. 2). The low-level winds were southerly at 5-10 m sec^{-1}, veering to west-northwesterly and becoming very strong aloft. Storm motion vectors for the two time periods are indicated by the points V_1 and V_2. The effect of the storm movement was to increase (roughly double) the relative southerly flow, and turn the relative mid-tropospheric winds to westerly. The environmental wind shear from 3 to 12 km is computed from Fig. 4 to have been 8.0×10^{-3} sec^{-1}. Wind shears computed similarly from other undisturbed soundings in the vicinity of the storm were slightly lower, with an average for five soundings (three released at 1530 and two at 1700) being 6.5×10^{-3} sec^{-1}. This is large enough to characterize the storm environment as being severely sheared (Marwitz, 1972c).

The 1541 Sterling sounding is plotted in Fig. 5. The large dot at 720 mb indicates conditions at cloud base (beneath the pedestal cloud--see Sec. 6) as determined by the Queen Air aircraft flying just below cloud base in the main updraft of the Fleming storm (temperature 8C, mixing ratio 10 g kg^{-1}). Sterling, though in the moist surface air for most of the day, was on the warm side of an

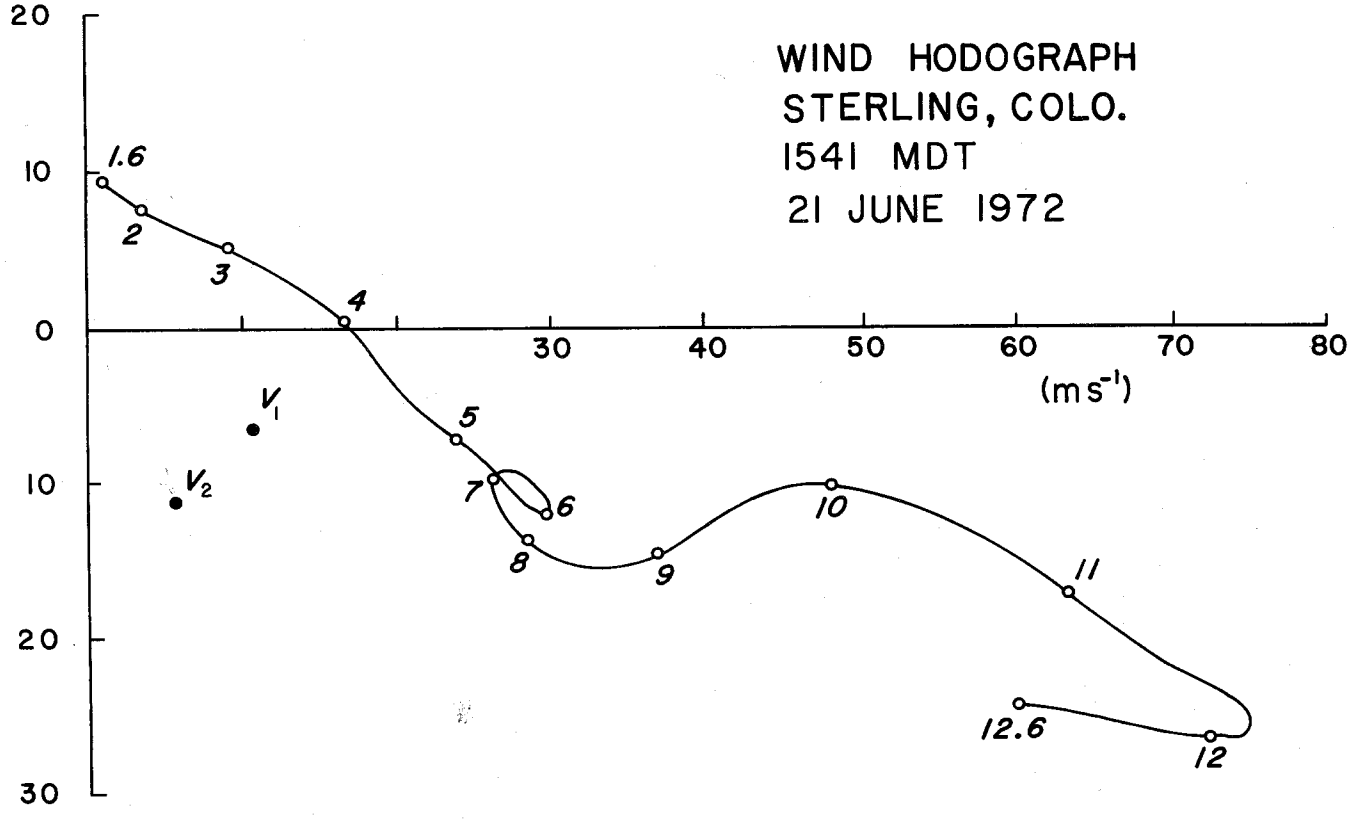

Fig. 4 Hodograph of 1541 MDT rawinsonde from Sterling on 21 June 1972. Storm motion vectors for the periods before and after 1555 are labeled V_1 and V_2 respectively. With respect to the storm in its severe stage (place origin of hodograph at V_2), the mid-tropospheric winds were westerly and the low-level winds were southerly at 15-20 m s^{-1}. The sounding terminated at the 12.6 km altitude.

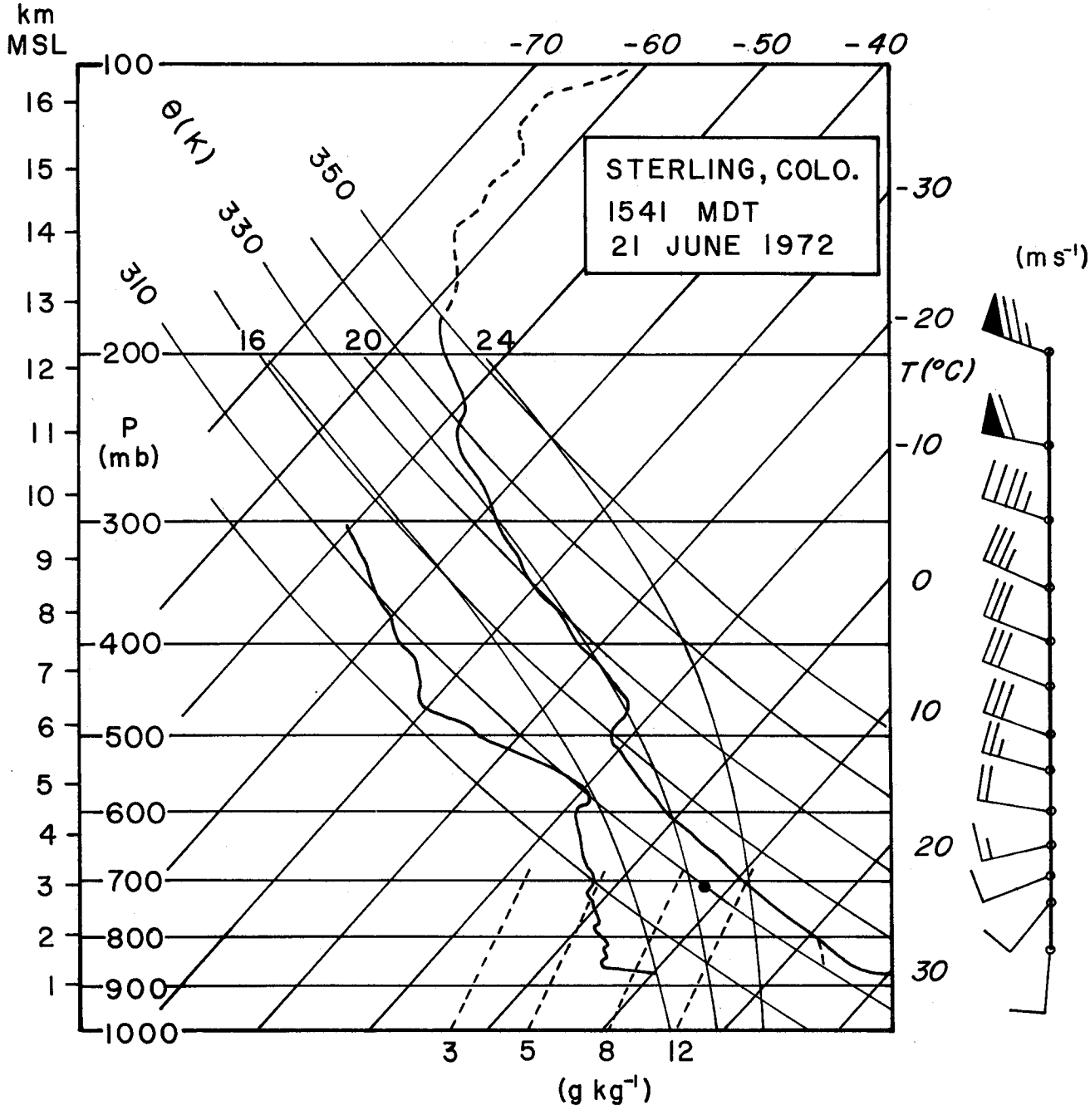

Fig. 5 Temperature and dew point plotted on skew T - ln p diagram for the 1541 MDT sounding from Sterling on 21 June 1972. The sounding was terminated at 190 mb, and the dashed upper part of the temperature trace is added from an 1830 Sterling sounding which matched very closely the 1541 mid-tropospheric temperature profile. The dashed lower part of the temperature curve represents environmental conditions actually encountered by the Fleming storm (see text). The heavy dot at 720 mb indicates saturation conditions in the storm updraft determined by an aircraft flying just below cloud base.

east-west surface temperature gradient; only 30 km farther east the low-level temperatures were some 5C cooler. It was this cooler and slightly more humid air, shown as the lower dashed part of the temperature sounding, that was in a position to enter the inflowing branch of the storm circulation, and was detected by the Queen Air at cloud base. An extremely shallow layer with high mixing ratio is indicated near the surface in Fig. 5, a situation that is not uncommon in northeastern Colorado. The implication is strong here, as in cases previously reported (Marwitz, 1972a, 1973a) that the storm draws its core updraft air from a shallow layer near the surface.

Although conditions in the low-level southerly flow over Sterling were not representative of the actual storm environment, conditions above 800 mb at Sterling (Fig. 5) were in agreement with the multi-level aircraft measurements. Thus, we are confident that the air entering the cloud base was about 4C colder than the environment at the same altitude (the virtual temperature deficit was 3C). Evidence for a negative buoyancy at cloud base is well documented for storms in the northeast Colorado area (Marwitz, 1973a). Upon rising through cloud base an unmixed parcel would have ascended the pseudo-adiabat with an equivalent potential temperature θ_e of 340K (or wet bulb potential temperature of about 21C), it would have reached its level of free convection at 640 mb, and thereafter would have experienced a temperature excess of about 4C over the far environment.

The nature of the environmental sounding in Figs. 4 and 5 suggests two reasons why the Fleming storm was able to maintain a quasi-steady state. First of all, the convective Richardson number (Ri), defined by Moncrieff and Green (1972) as the ratio of available potential energy due to buoyancy to available kinetic energy due to shear, would have been small. According to Moncrieff and Green, a small value of Ri implies that the inflow may be properly matched to the magnitude of the buoyant updraft and this enables the updraft to be persistent.

In this respect the Fleming storm was unlike most storms in northeast Colorado which tend to be characterized by larger Ri owing to high instability combined with smaller shear. Such storms may still be vigorous but individual storm cells are unable to attain a steady state because the inflow is insufficient to sustain the vigorous updrafts that develop in the presence of large buoyancy. Another factor encouraging the maintenance of a steady state was the large negative buoyancy in the inflow below cloud base. This was characteristic not only of air originating near the ground but also of air originating from all levels in the lowest 3 km (AGL). All of this air needed to be lifted more than 2.5 km before it reached its level of free convection. This had the effect of inhibiting premature release of convective instability as the inflow approached the main updraft and so the Fleming storm preserved a single isolated updraft instead of having a succession of new updrafts break out on the flank of an existing updraft as in the more common multicell hailstorms described, for example, by Dennis, et al, (1970) and Marwitz (1972b). Maintenance of a strong and persistent updraft is regarded as important from the point of view of hail growth because, as we show later, it can provide the opportunity for hail embryos to recycle and grow into large hailstones in an updraft whose cloud water has not suffered from excessive depletion.

5. Airflow near the storm in relation to its radar structure

(a) The three-dimensional radar structure

Details of the radar echoes from the Fleming storm are illustrated in Fig. 6, showing PPI displays at four altitudes. The period shown here, 1552-1553, is near the time the storm made its turn to the right, when the extensive hail swath began and large hail started reaching the ground. Shortly after this the storm moved out of range of the Grover radar. Although the echo configuration shown here had been well established for only 20 min or so, the less detailed

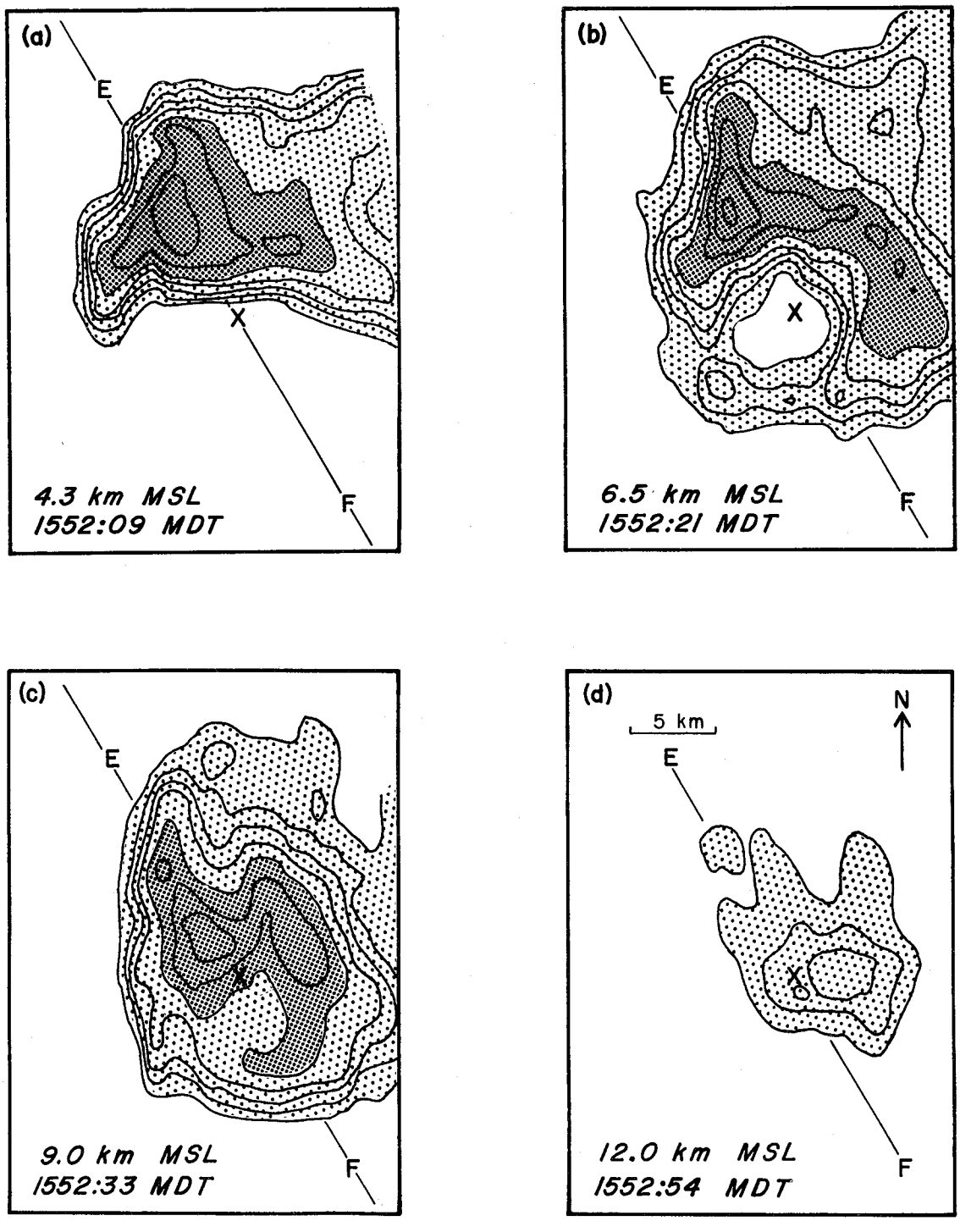

Fig. 6 Quasi-horizontal sections at four altitudes showing the three-dimensional pattern of radar reflectivity for the Fleming storm at 1552-1553 MDT. Reflectivity contours are at 5 dBZ intervals. Areas in excess of 30 and 50 dBZ, respectively, are stippled thinly and thickly.

but still quantitative CHILL radar data confirm that the storm maintained an intense single-cell structure resembling Fig. 6 for at least several hours.

Figure 6a shows the lowest scan available at this time, at a mean altitude of 4.3 km (all heights MSL in this paper). The heavily shaded area shows the region where the reflectivity exceeded 50 dBZ. For ease of description, we shall refer to this general area to the north of the vault as the hail cascade. The weakly developed hook echo on the west side withdrew northward with decreasing altitude and was not in evidence near the surface (surface level is 1.4 km). Figure 6b at 6.5 km shows echo completely surrounding the vault, which was situated to the south of the precipitation wall aligned east-west in Fig. 6a. The echo surrounding this bounded weak-echo region is composed of the hail cascade on the north with some of it wrapping around from the east, and the embryo curtain on the south--the giant curved streamer of Browning's (1965b) study. By 9.0 km (Fig. 6c) the radar was scanning over the top of the vault, but a weakness in the reflectivity pattern remained there. Fig. 6d shows the rather rounded echo near the top of the storm, and its position over the vault.

The vertical cross-section in Fig. 7 has been constructed along the line EF in Fig. 6. As will be seen, this is approximately along the mean inflow direction. It shows the vertical continuity between the PPI's of Fig. 6 and illustrates more dramatically the supercell structure, including the large forward overhang and the weak-echo vault located (as shown presently) above the organized updraft. Similar supercell features are well-documented for a number of other recent cases (e.g., Marwitz, 1972a,c; Chisholm, 1973; Foote and Fankhauser, 1973; Nelson and Braham, 1972). We will return to more details of the radar structure after discussing other types of observations.

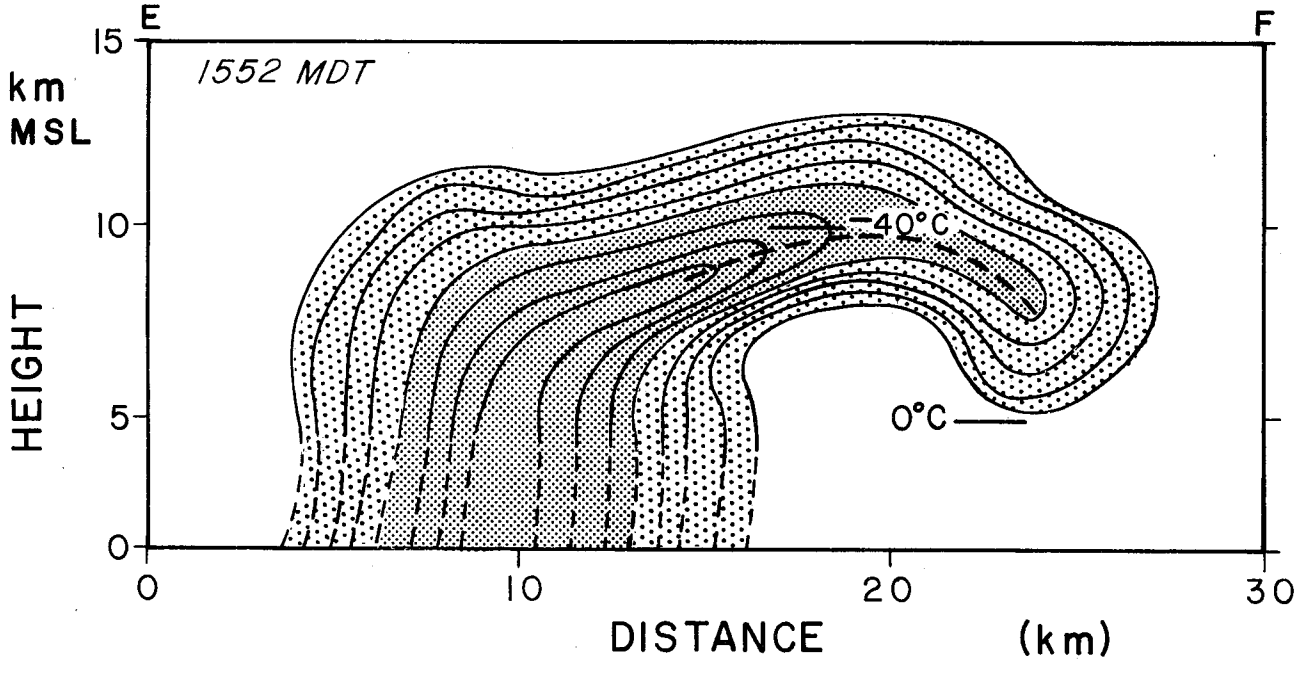

Fig. 7 Pattern of radar reflectivity for the Fleming storm in a vertical section along EF in Fig. 6. Contours and shading are as in Fig. 6. The resolution in this figure, as in Fig. 6, is limited by the 1-deg beamwidth and by the 1-sec time integration while scanning in azimuth at 1 deg sec^{-1}. The Grover radar was located about 95 km west of the storm.

(b) Airflow near the storm at low levels

The track of the Buffalo aircraft as it flew around the storm in the sub-cloud region at 2.3 km is shown in Fig. 8. The track has been adjusted for the motion of the storm (from 335 deg at 12 m sec^{-1}), and is positioned with respect to the low-level CHILL PPI echo at 1634 (shown stippled), some 40 min after the Grover radar data in Figs. 6 and 7. The hatched region south of the strong echo marks the extent of the forward overhang aloft as determined by the DC-6 tail radar 5 to 8 min later. This echo overhang includes both the vault region and the embryo curtain surrounding the vault on its southern boundary. Horizontal wind vectors relative to the moving storm are plotted at 15-sec intervals along the track (the method of track adjustment and the wind-measuring capabilities of the aircraft discussed here have been summarized by Foote and Fankhauser (1973)). The east-west leg of the Buffalo track along the southern flank of the storm has also been replotted below to show winds with respect to the ground (note the change of vector plotting scale).

The dashed line under the echo overhang indicates part of the relative track of the Queen Air as it flew in the organized updraft a few hundred meters below cloud base from 1510 to 1630 (cloud base altitude $\sim$ 2.8 km). The traverses were flown roughly parallel to the wall of precipitation to the north, and only the last three of the twelve legs that were flown are indicated. The aircraft turned at the end of each traverse after losing detectable updraft, so that the east-west extent of the updraft was a few kilometers less than the limits of the Queen Air track shown in Fig. 8. Unlike the Buffalo, the Queen Air was not properly equipped to make quantitative updraft measurements. Estimates could be made, however, by flying at constant attitude and power setting, and monitoring the aircraft's rate of climb. In this way the updrafts for the last several passes

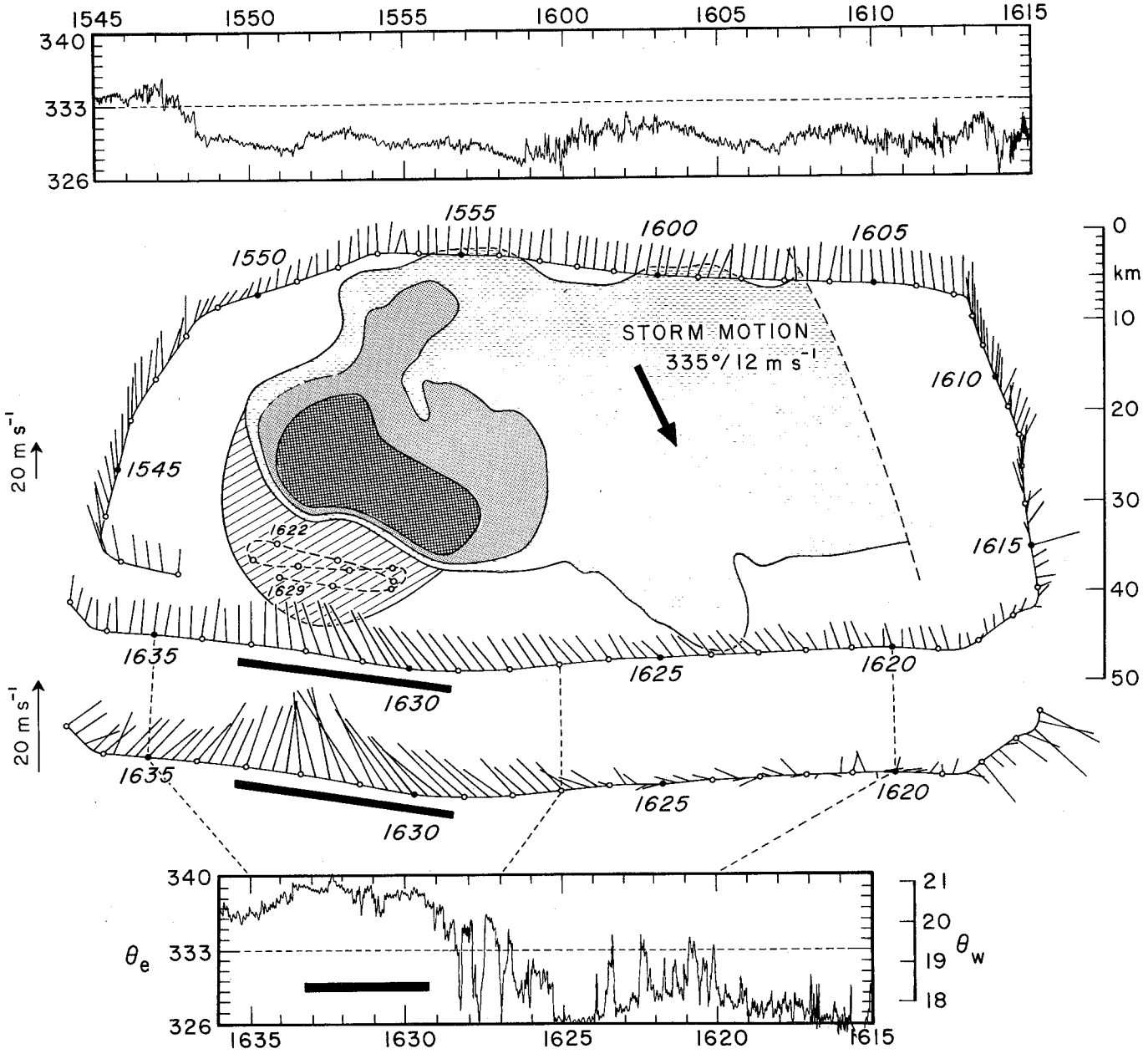

Fig. 8 Ground track of the Buffalo aircraft flying at an altitude of 2.3 km MSL, plotted relative to the moving storm. Horizontal wind vectors relative to the storm are shown along the track, with the convention that the tail of the vector lies on the track. The offset segment of the track displays winds with respect to the ground (note change in vector scale). The bar denotes region of updraft detected by the Buffalo. The shaded region is the low-level PPI echo from the CHILL radar at 1634 MDT (the contour levels are 20, 32, and 45 dBZ; the position of the inner contours is not well established). The hatched region indicates the extent of the echo overhang aloft. The dashed line shows part of the Queen Air track as it flew in the main updraft just below cloud base. Panels at the top and bottom show the equivalent potential temperature of air encountered by the Buffalo.

were estimated to be 10-15 m sec^{-1}. The maximum updraft occurred roughly in the center of the Queen Air track, directly beneath the vault. The visual appearance of the cloud base containing the organized updraft is shown in Fig. 9. The broad, flat cloud base adjacent to a dark curtain of precipitation is unmistakable, and as pointed out by Marwitz, et al (1972), can be identified visually from a great distance. The cloud base maintained this general appearance over the 90 min period of observation, and a strong smooth updraft was encountered in the same relative location on each of the twelve Queen Air traverses during this time.

The bar along the Buffalo track in Fig. 8 from 1629 to just after 1633 marks the extent of the updraft along this pass through the inflow. The maximum updraft there was about 3 m sec^{-1}, and occurred at the 1631 position, just upstream from the maximum determined by the Queen Air. We notice that the 16 km width of the updraft determined by the Queen Air is only two-thirds of that measured in the inflow by the Buffalo, and that this reduction in width is consistent with the confluent relative winds shown along the Buffalo track. The winds in the inflow-sector displayed with respect to the ground (lower offset track in Fig. 8) show an even more marked confluence than the relative winds, with values in excess of 20 m sec^{-1} (corresponding to relative inflow magnitudes as great as 35 m sec^{-1}). The Queen Air winds at cloud base (not shown) are in good agreement with the Buffalo inflow winds, both in their magnitude and predominant direction and their preservation of the marked confluent feature. The evidence is quite strong that horizontal momentum was being rather strictly conserved from the Buffalo's position in weak updrafts under the southern edge of the storm to the center of the strong updrafts at cloud base level. The acceleration from the 5-10 m sec^{-1} low-level environmental flow to the 20 m sec^{-1} winds measured near the updraft implies the

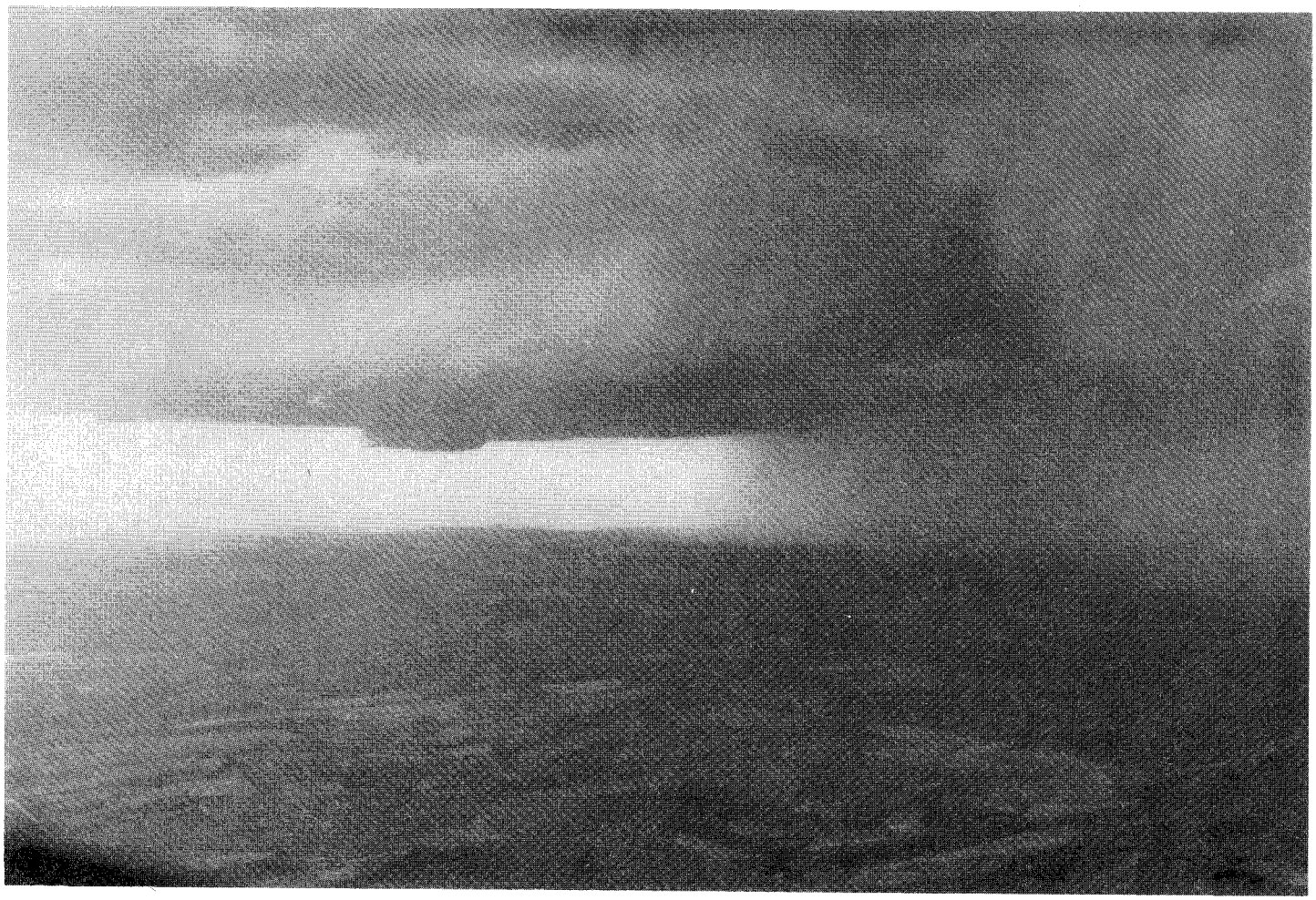

Fig. 9 Photograph looking to the northwest at 1545 MDT showing the broad cloud base associated with the organized updraft of the Fleming storm. A dark wall of precipitation is seen on the right. The small "collar cloud" attached to the otherwise flat cloud base, occurring in the center of the strong updraft, was not a persistent visual feature.

existence of a pressure deficit there of about 1.0-1.5 mb. Pressure deficits associated with mesolows beneath updrafts are usually smaller than this (e.g., Foote and Fankhauser, 1973; Barnes, 1974).

The panels at the top and bottom of Fig. 8 show the equivalent potential temperature θ_e of air encountered by the Buffalo at 2.3 km. Values averaging 339K are shown in the strong inflow, with peaks to 340K. Identical values of θ_e were measured by the DC-6 at an altitude of 2.7 km during its pass through the inflow some 7 min later, although the high values occurred over a shorter distance. Equivalent potential temperatures measured in the strong updraft by the Queen Air were about 1 deg higher, but this difference is probably within the accuracy of the measuring instruments. Reference to the sounding of Fig. 5 shows that this air could have originated only very near the surface.

On the northern side of the storm the values of θ_e were only slightly lower than the environmental value for this altitude of 331K. Although the air motion there would indicate that this air had participated in the storm circulation and exited to the rear, its θ_e -value is not particularly helpful in determining its origin. Not until the Buffalo encountered the region of the turbulent gust front, from about 1615 to 1619, were particularly low values of θ_e detected. Equivalent potential temperatures there of 326-328K can be found only in the 500-600 mb layer in appropriate soundings; presumably this air had descended from that altitude (low values of θ_e occurred also in the outflow on the western flank of the storm but here the Buffalo track had been above the level of the cold outflow). By 1627 the Buffalo was in a transition region where the horizontal winds were beginning to respond to the proximity of the main updraft, and where θ_e while showing a gradual rising trend also showed large short-term fluctuations associated

with considerable turbulent mixing of air from different levels. The transition from low to high θ_e (dry to moist air) on the east side of the inflow was much more abrupt at the level of the DC-6 (2.7 km), and the contrast was greater yet at the Queen Air position, where further lifting and convergence tightened the gradient between ambient air and moist updraft air. A similar sub-cloud structure is shown in the measurements of Foote and Fankhauser (1973).

As a result of the movement of the storm toward the south-southeast, the relatively slow-moving air in the region of the Buffalo track from about 1620 to 1627 had a component of motion toward the storm (Fig. 8). The presence of a gust front, part of which was traversed by the Buffalo at about 1618, would have forced this air upward through its condensation level, leading to the secondary and higher cloud base observed in this region. It was not possible for this air to undergo penetrative convection, however, for after passing into the cloud it would always have been some 1-2C cooler than the environment. It probably rose over a relatively shallow gust front and then participated in the storm downdraft.

(c) Airflow near the storm at middle levels

Fig. 10 shows an example of the wind field near the storm in the middle troposphere. The track and winds are those of the C-130 flying at 7.9 km and equipped with a Doppler Navigation system. The radar data, similar to that of Fig. 8, is a low-level CHILL scan for 1634, along with a PPI composite from the DC-6 tail radar showing the embryo curtain at an altitude of 7.5 km. As before, the aircraft track has been adjusted for the storm movement and the wind vectors are shown in a coordinate system moving with the storm. The main point here is the blocking effect of the storm on the ambient mid-level winds, as highlighted by the streamline analysis showing an upstream stagnation point and the airstream

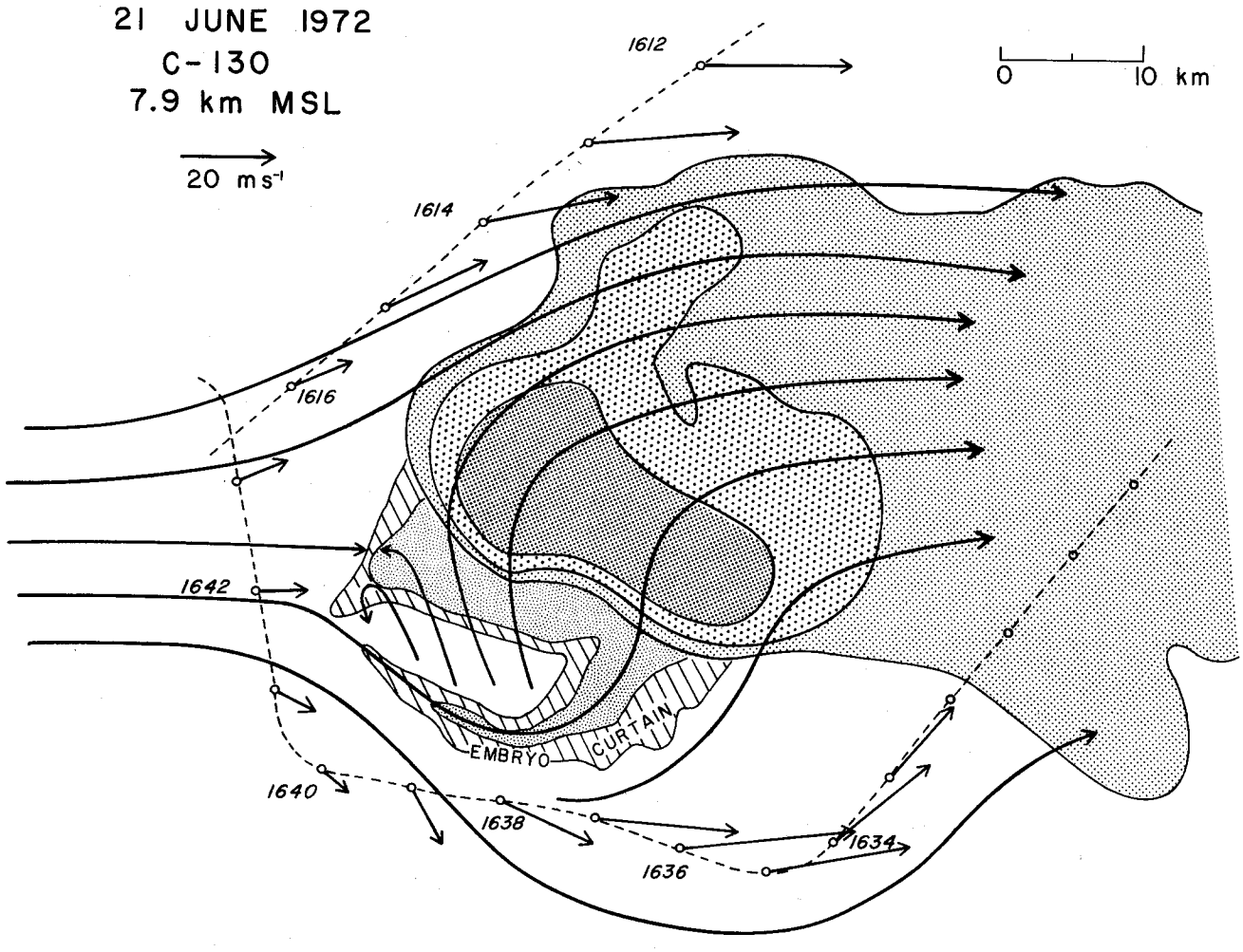

Fig. 10 Winds measured by the C-130 aircraft as it flew around the Fleming storm at 7.9 km MSL (track and winds shown relative to the storm). The radar data consists of a low-level PPI from the CHILL system (as in Fig. 8), and a horizontal composite from the DC-6 radar showing the overhanging echo at an altitude of 7.5 km. The streamline analysis emphasizes the blocking flow with a forward stagnation point.

parting around the storm. This phenomenon, first postulated by Newton and Newton (1959), has also been reported by Fujita and Arnold (1963) and Fankhauser (1971). Although there is little direct evidence to support the streamline analysis in the interior of the storm (the aircraft Doppler winds, for example, are not reliable near precipitation), we shall later argue strongly for the main features shown here, such as the continuing southerly flow in the updraft rising within and to the north of the vault and the flow along the axis of the embryo curtain.

6. Visual appearance of the hailcloud and its relation to the radar structure

A vertical section of the Fleming storm through the radar vault and oriented along the mean inflow direction is shown in Fig. 11 for the same time period emphasized in the previous section, 1630-1640 MDT. The diagram shows data from both radar and visual observations. The reflectivity pattern on the southern flank of the storm, including the embryo curtain and the vault structure, was determined by the X-band tail radar on the DC-6 aircraft as it flew along the southern boundary of the storm (aircraft positions are indicated in the figure). The northern part of the storm could not be detected by the DC-6 radar at this time owing to severe attenuation, so this region was reconstructed from data obtained at the same time from low-level CHILL scans and from the airborne radar observations made 10 min earlier as the DC-6 flew around the northern side of the storm. As shown in the previous section, the base of the strong updraft was located directly beneath the vault, and relative air motion vectors there and in the inflow are sketched at representative positions of the Queen Air and Buffalo in Fig. 11.

The embryo curtain is revealed in Fig. 11 as a more slender feature than in Fig. 7. Much of this difference, as well as some of the indicated change in the maximum height of the vault, can be attributed to the finer resolution of the air-

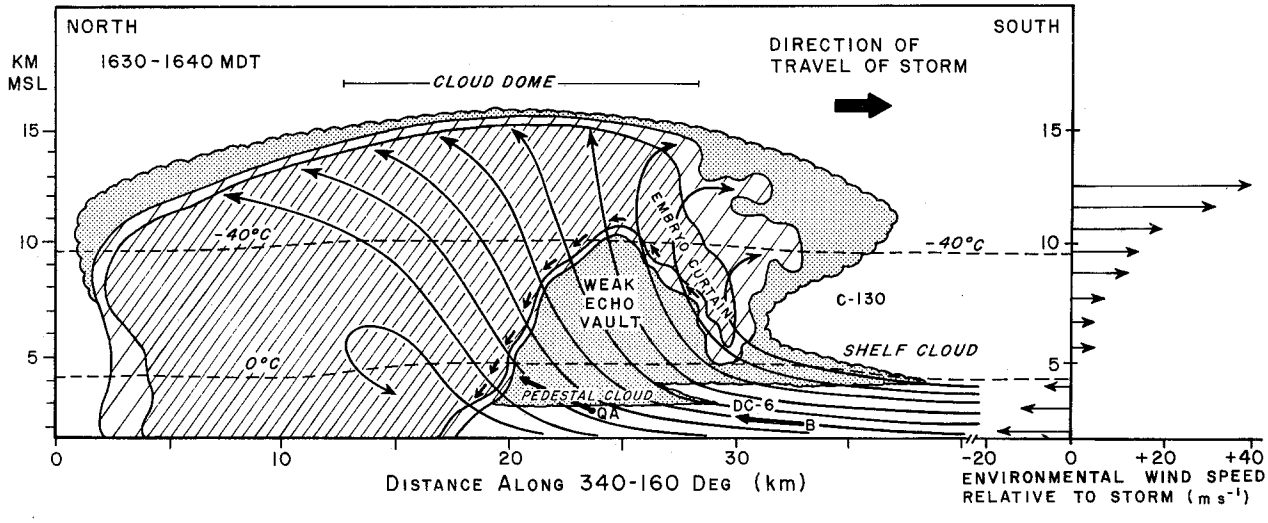

Fig. 11 Vertical section showing features of the visual cloud boundaries of the Fleming storm at 1630-1640 MDT superimposed on the pattern of radar echo derived as explained in the text. The section is oriented in the direction of travel of the storm, along the straight line drawn in Fig. 14. Two levels of radar reflectivity are represented by different densities of hatched shading. Areas of cloud devoid of detectable echo are shown stippled. Location of the four instrumented aircraft are indicated, viz: C-130, QA (Queen Air), DC-6 and B (Buffalo). Bold arrows denote wind vectors in the plane of the diagram as measured by two of the aircraft (scale is only half that of winds plotted on right side of diagram). Short, thin arrows skirting the boundary of the vault represent a hailstones trajectory (discussed later). The thin lines are streamlines of airflow relative to the storm drawn to be consistent with the other observations. To the right of the diagram is a profile of the wind component along the storm's direction of travel, derived from a Sterling sounding 50 km south of the storm.

borne radar at close range compared with the Grover observations. The outer contour of the DC-6 radar data corresponds to a reflectivity of 0 dBZ at a distance of 10 km and -20 dBZ at 1 km. The inner contour is 16 dB higher. Thus, Fig. 11 indicates that the reflectivity in the vault was everywhere less than 1 $mm^6 m^{-3}$, thereby imposing limitations on the size and concentration of particles that can have been present there. For example, at concentrations of 10-100 m^{-3}, perhaps typical of small graupel (Musil, et al, 1975), the particles can have been no larger than about 1 mm in diameter. Similar observations of the reflectivity in weak-echo regions have been made by Grandia (1973).

There are several important visual features depicted in Fig. 11. One is the cloud top which was photographed at 1636 from the Queen Air (Fig. 12). This photograph, obtained looking from the west about 35 km from the storm, shows that the main storm top, reaching a height of 15.5 km, had the appearance of a large, smoothly rounded dome. As shown by Cunningham (1960) and Roach (1967), such a cloud dome is a characteristic feature of vigorous, quasi-steady storms. Before the onset of the severe right-moving stage of this storm, no such dome had existed; instead, until about 1540 there had been a rather lower cloud top (13.0 km) composed of numerous discrete and evolving turrets. The location of the lateral cloud boundaries shown in Fig. 11 was obtained fairly precisely on the southern edge of the storm from the photograph in Fig. 12 and from photographs taken on board the C-130 and from Grover. Evidently the embryo curtain was located just within the cumuliform cloud boundary.

There were two, perhaps even three, different cloud bases on the southern flank of the storm, the principal two being sketched in Fig. 11. Air entering the strongest part of the updraft passed through a pedestal cloud, while air ascending farther south passed through a larger and more diffuse cloud base at

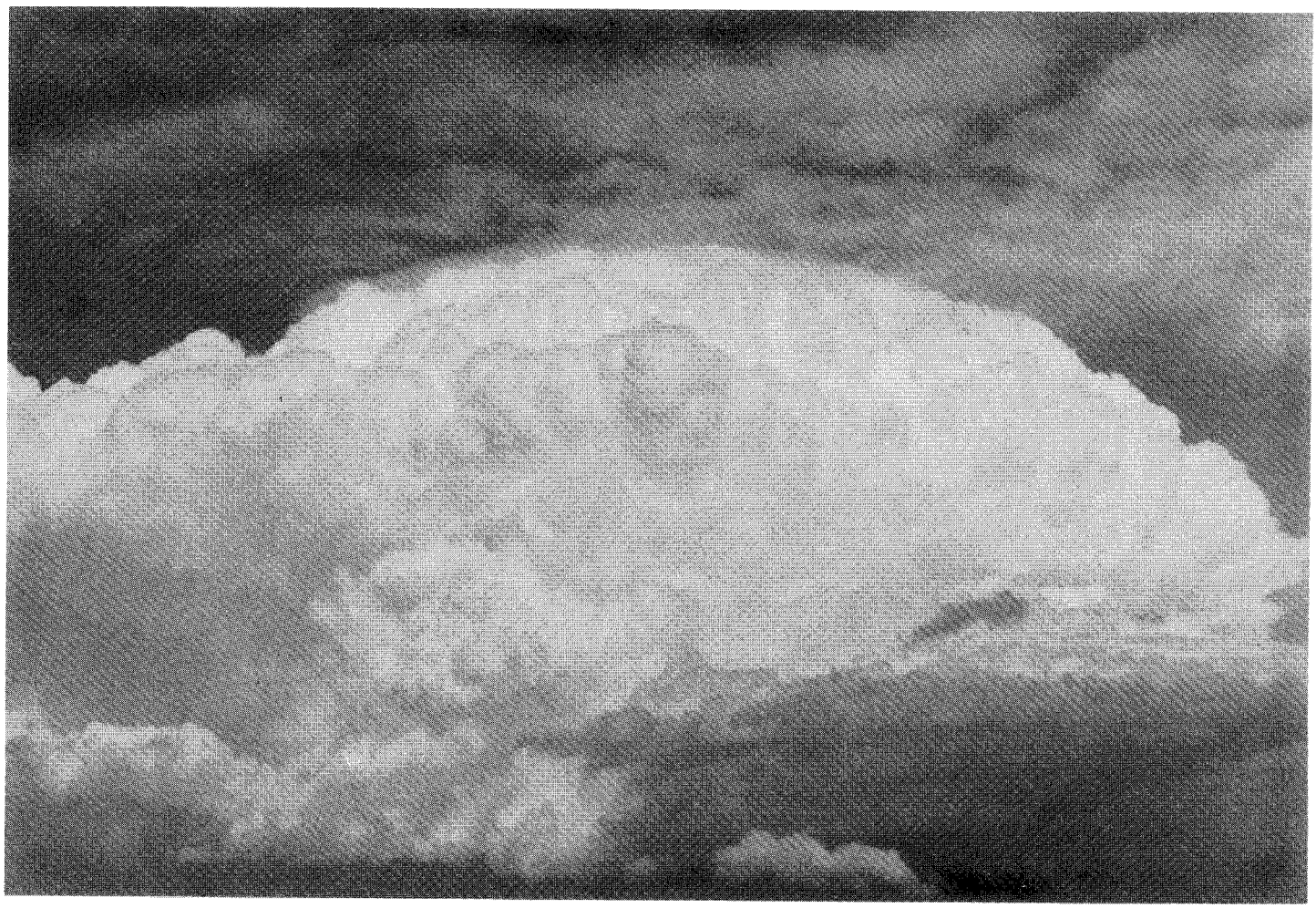

Fig. 12 Photograph of Fleming storm taken from a position 35 km west of the storm at 1636 MDT showing vigorous turrets on the west flank of the storm and a smoothly-shaped dome at the top of the storm.

a higher level, here called a shelf cloud. The southwestern edge of this shelf cloud can be seen in Fig. 3 at 1615. The different cloud bases existed because the air entering the pedestal, which, as shown in the previous section, must have originated close to the ground, had a substantially lower condensation level than air originating somewhat higher up owing to its higher mixing ratio and lower potential temperature (Fig. 5). A photograph of the pedestal cloud taken from the east-southeast near 1637 is shown in Fig. 13. Detailed photogrammetry using a large number of photographs revealed that the pedestal cloud was oval-shaped in plan view, as mapped in Fig. 14. Most of it was situated directly beneath the vault but it had a toe extending toward the southeast along the direction of the inflow, and it is this extension that is seen in profile in Fig. 13 and sketched in Fig. 11. The upper edge of this part of the pedestal forms a streamline separating regions of air having different lifted condensation levels (LCL's). The shallow slope of this streamline is in agreement with the Queen Air and Buffalo observations. The overall flow pattern illustrated in Fig. 11 is justified more fully in the next section.

The existence of an abrupt lateral boundary on the eastern edge of the pedestal, as seen in Fig. 13, is in agreement with aircraft measurements indicating a sharp gradient of θ_e and LCL there. These gradients resulted from the large differential vertical motion. The higher dark cloud base seen just to the north (right) of the pedestal corresponds to a region of very weak updrafts, and may be similar to the cloud vault described by Marwitz (1972c). It was this region that was discussed in the previous section in terms of the forced lifting of stable air by a shallow gust front. The scud cloud shown in the right hand side of the photograph ahead of the cloud vault is thought to be a result of the mixing of moist and dry air parcels detected by the Buffalo on the eastern shoulder of the inflow.

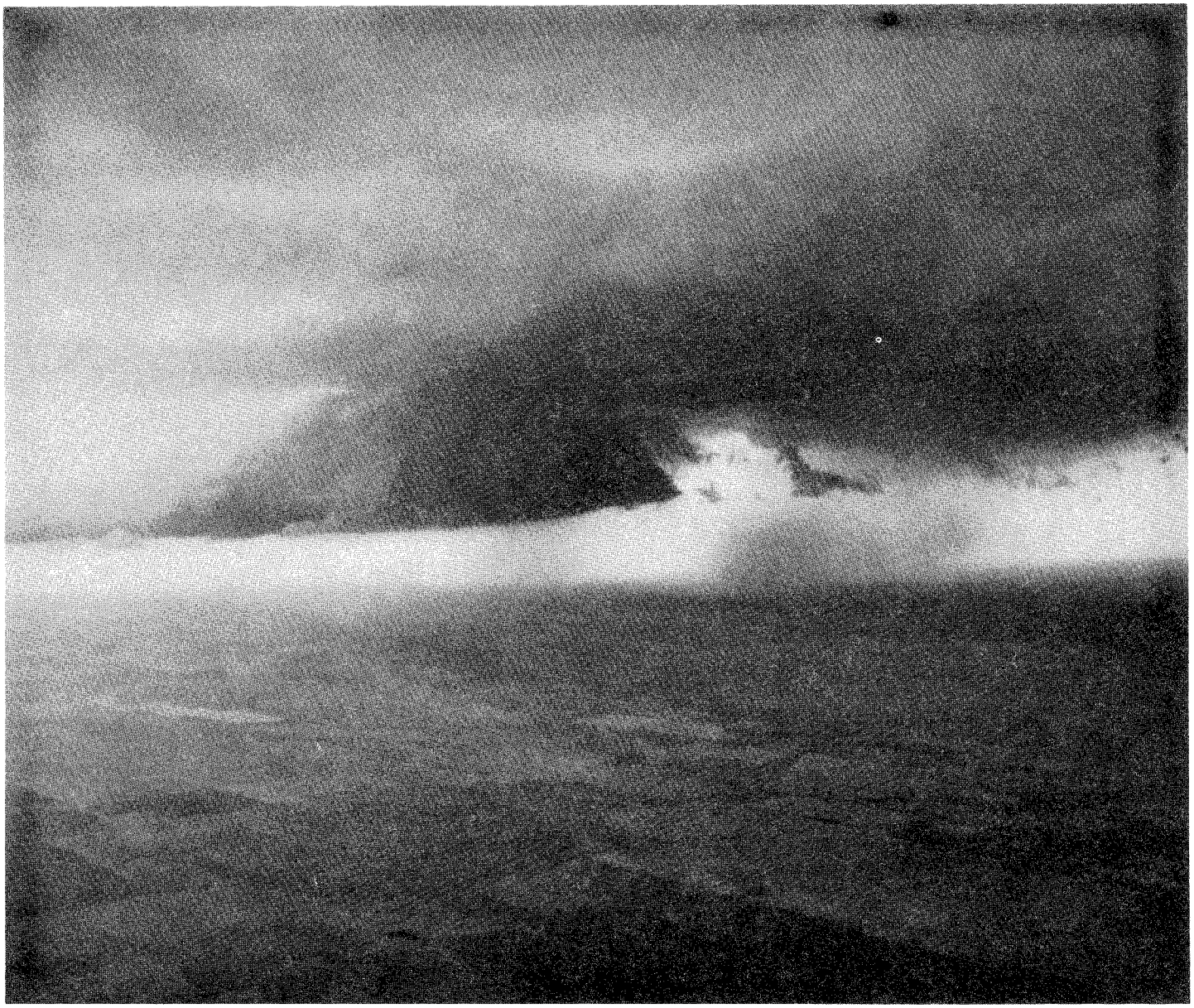

Fig. 13 Photograph of pedestal cloud in the Fleming storm at 1637 MDT showing a flat base and sloping upper boundary. Scud is visible in the right side of the photograph, and blowing dust is evident near the ground. The location from which the photograph was taken is plotted in Fig. 14. See text for further details (photograph courtesy of B. B. Phillips).

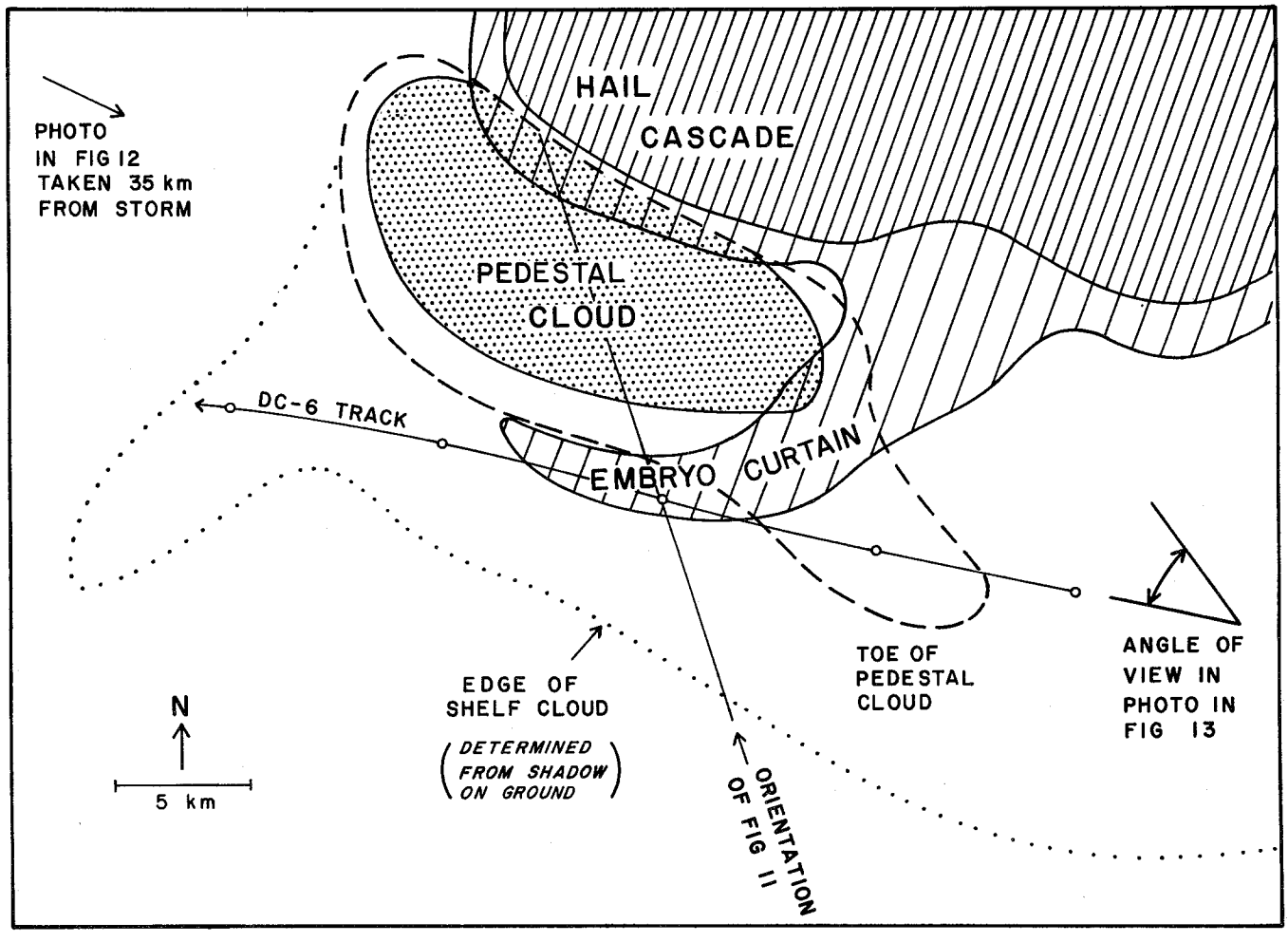

Fig. 14 Plan view of the two main cloud bases in the Fleming storm at 1630-1640 MDT shown in relation to the pattern of radar echo at 3.5 and 5.5 km MSL (thickly and thinly hatched) as derived from the DC-6 tail radar. The horizontal extent of the pedestal cloud where it entered the base of the shelf cloud at 4 km MSL is shown heavily stippled. The base of the pedestal cloud, at 2.8 km MSL, had a slightly greater extent especially where it extended as a toe toward the southeast (dashed outline). The location of the pedestal cloud has been reconstructed from the photograph in Fig. 13 and from a succession of photographs taken along the track of the DC-6 aircraft. The extent of the shelf cloud is indicated by the dotted curve. It has been determined from the position of the shadow on the ground and also from the photograph in Fig. 3 and time-lapse photographs from a ground-based camera at Grover.

Indeed, judging from measurements of θ_e presented in Fig. 8, some of the air in this region had descended from higher levels, perhaps in association with virga that was present. In that case, some of the air near the scud cloud was recycling and entering the cloud for the second time.

7. A two-dimensional model of the updraft in relation to visual and radar features of the storm

Before considering the flow in three dimensions, we first discuss some of the updraft features in the cross-section of Fig. 11. Although the flow of air around the cloud at middle levels was an essentially three-dimensional feature, as shown by the C-130 data in Fig. 10, and although the updraft itself became decidedly three-dimensional as it interacted with air near its lateral boundaries and as it diverged horizontally near its summit, the flow in a section such as Fig. 11 is thought to be a useful and representative picture of the general flow pattern within the lower and middle portions of the main updraft.

The thin lines in Fig. 11 representing streamlines relative to the storm were shown in the previous section to be consistent with some of the visual cloud features and aircraft measurements. The form of these streamlines is, as we shall show, also consistent with the shape of the radar echo; however, before elaborating on this, it is necessary to introduce a possible alternative interpretation of the airflow in part of the storm (Fig. 15) which is also consistent with many of the observed features. Although there are important differences which we shall discuss presently, the airflow models in Figs. 11 and 15 are similar in regard to the broad sweep of the updraft, with a continuing component from the south in the updraft core as well as in the inflow. This is consistent with the wind measurements from the sub-cloud aircraft. It is consistent too

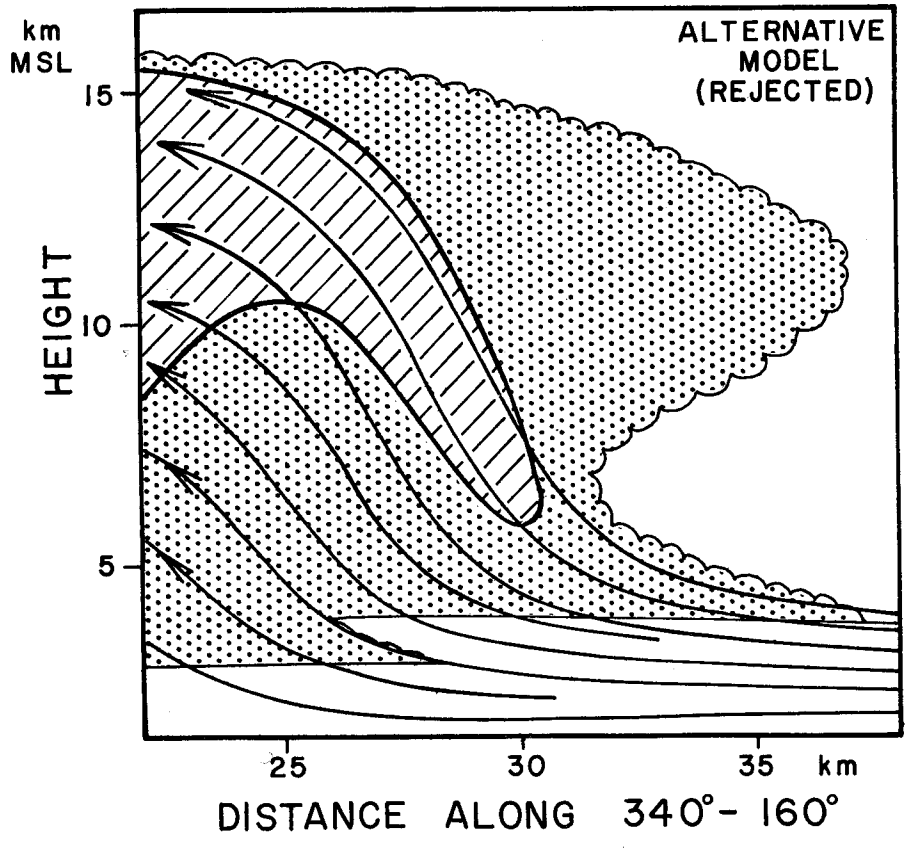

Fig. 15 Alternative model of the airflow in the region of the vault and embryo curtain. For reasons discussed in the text this model is rejected in favor of the version in Fig. 11.

with the observed slope of the upper edge of the pedestal cloud which must have been a relative streamline. A southerly component of motion in the updraft is also necessary to account for the observed slope of the hail cascade descending to the ground on the northern boundary of the vault. Preservation of the southerly inflow momentum within the updraft itself has been demonstrated in a similar kind of storm by means of radar-tracked chaff trajectories (Marwitz, 1972c). The same result was observed by tracking chaff in the present storm before its transition to the severe right-moving stage (Marwitz, 1973a).

The model in Fig. 15 is different from that in Fig. 11 only with respect to the flow in the embryo curtain. The difference may look slight but it is physically important since it implies two distinct mechanisms for the growth of hailstone embryos. The model in Fig. 15 resembles that proposed by Dennis and Musil (1973) and Danielsen, et al (1972). It assumes that the particles in the embryo curtain have been grown "from scratch" in rising from cloud base; in other words, the lower tip of the embryo curtain is considered to be a "first echo." While it is possible that such a model has some validity in the case of multicell storms, and possibly also in the case of supercell storms exhibiting an unbounded weak-echo region, we consider such an explanation to be invalid when the weak-echo region is in the form of a vault bounded by a distinct embryo curtain of the kind observed here. The lower tip of the embryo curtain in Figs. 11 and 15 is in fact within 1 km of the appropriate cloud base. Taking an updraft of 5-10 m s^{-1} between cloud base and the tip of the embryo curtain (consistent with our analysis in Sec. 8) gives a time of only 100-200 s, which is far too short for growth from the aerosol of particles capable of giving detectable echo. A similar argument was used by

Young and Atlas (1974) in their analysis of another supercell storm.

The more appropriate airflow model for the kind of storm discussed here is thus the one shown in Fig. 11. It resembles that proposed by Browning and Ludlam (1962) and later applied to severe Oklahoma hailstorms (Browning, 1965b). It assumes that the embryo curtain consists of recycling particles which formed earlier out of the plane of the figure and which describe a three-dimensional path as they circulate around the southern flank of the updraft. Strong evidence to support this view is presented in the next section. As is argued shortly, and is also argued by Young and Atlas (1974), the particles within the embryo curtain were being kept aloft within an updraft. Since the echo structure was essentially steady-state, the inner edge of the embryo curtain represented a trajectory envelope, with particles at the edge either rising or traveling out of the plane. In fact, we shall show they were doing both.

8. The motion and nature of precipitation particles in the embryo curtain and the proposed three-dimensional airflow structure

(a) Determination of the horizontal component of airflow around the embryo curtain

The storm, on entering its severe right-moving stage of development at 1550, maintained an essentially steady configuration with a characteristic echo pattern of the kind depicted in Figs. 6 and 7. Superimposed on the steady state pattern, however, were occasional pulsations. These were sometimes evident visually as cloud turrets protruding a little from the edge, but still forming a part of the main cloud mass (see Fig. 12). On radar the pulsations were evident as small regions of higher reflectivity ("hot spots") with dimensions of 2 or 3 km. These hot spots are not regarded as being

particularly important in themselves since the particles associated with them would probably have grown and traveled in essentially the same manner even if the overall updraft structure had been truly steady state. However, they are useful as tracers of the field of motion. Of particular value were the echo hot spots in the embryo curtain. Some of these could be traced as distinct entities for longer than 10 min, and therefore provided confident estimates of the velocity field in this part of the storm.

Figure 16 shows a set of tracings of the echo pattern from the Grover radar which reveals both the three-dimensional structure of the embryo curtain and the motion of a hot spot within it during the period 1543 to 1558. This corresponds to the period when the storm had just developed its supercell structure; soon afterwards it moved out of range of the Grover radar. The radar data included complete scan sequences once every minute, and enabled the motion of hot spots to be determined. Figure 16 (a-d) is a selection of PPI presentations close to the lower tip of the embryo curtain showing the position of a hot spot (X) at approximately 2-min intervals. The embryo curtain is seen to enclose the vault partially in Figs. 16 (b-d) and totally in Fig. 16a. The difference is a result of the sections in Figs. 16 (b-d) being marginally lower than that in Fig. 16a, so that they were a little beneath the base of the embryo curtain on the southwest side of the storm where the base of the curtain was highest.

Successive positions and velocities of Hot Spot X are plotted in Fig. 16f relative to the storm. The nearly circular dashed line represents the axis of most intense echo, passing through the embryo curtain on one side of the vault and through the hail cascade on the other. Hot Spot X was first identified

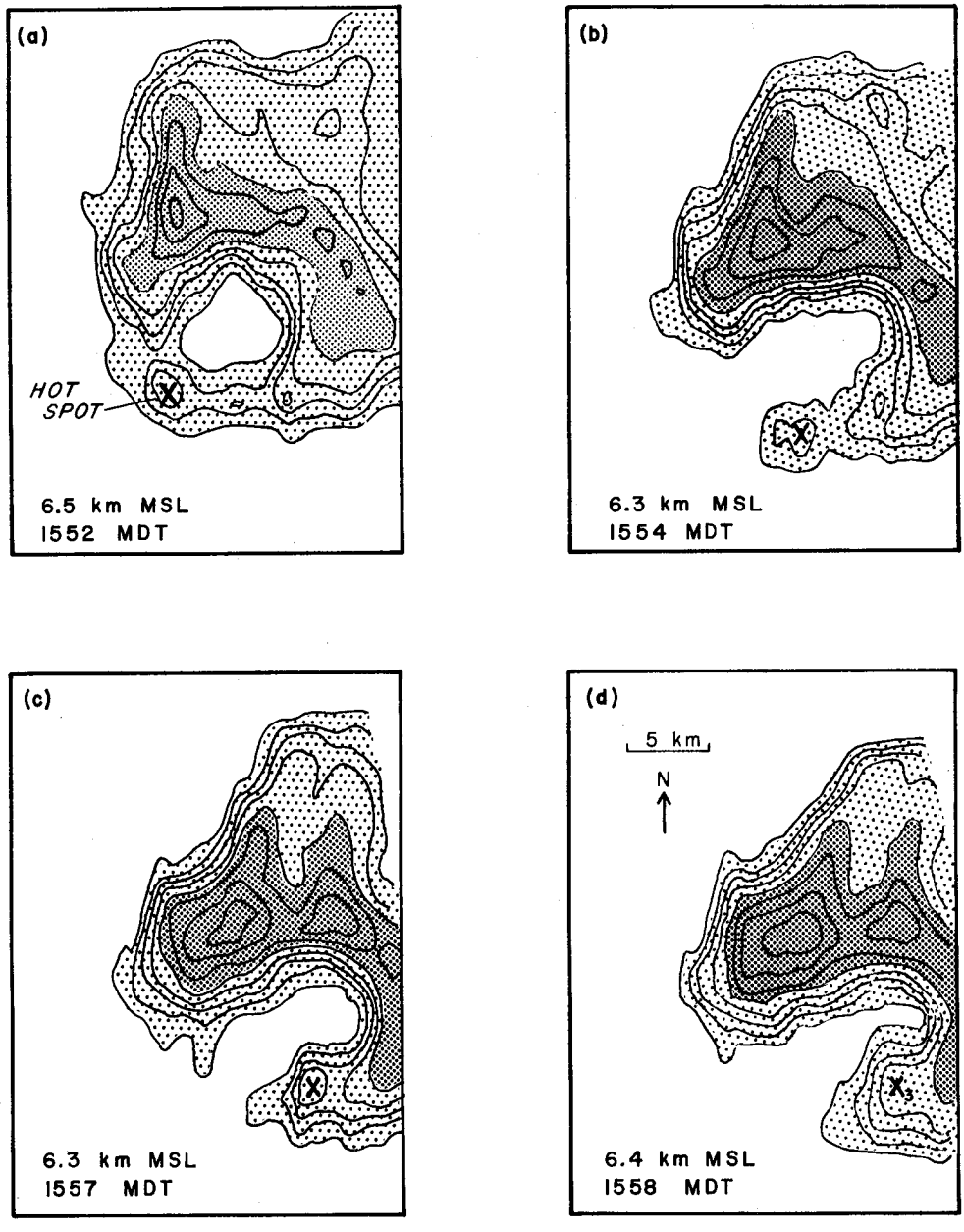

Fig. 16 Series of quasi-horizontal radar sections through the Fleming storm illustrating the nature and movement of an echo "hot-spot" (X) around the embryo curtain on the southern flank of the vault. Contours in most of the sections represent radar reflectivity in steps of 5 dBZ; areas with reflectivity in excess of 30 and 50 dBZ are stippled thinly and thickly, respectively. Figs. 16(a-d) show sections at 6.4 $\pm$ 0.1 km depicting the location of Hot Spot X at roughly 2-min intervals. Fig.16(e) is a similar section at 10.3 km which shows, protruding from the western flank of the main echo, the echo top from which Hot Spot X emanated. Fig.16(f) shows the motion of Hot Spot X (also Hot Spot Y) with velocity vectors relative to the storm (heavy arrows) positioned in relation to a dashed circle (AB) representing the axis of most intense echo bounding the vault. Also plotted in Fig.16(f) (thin arrows) are relative winds around the storm determined from the C-130 aircraft.

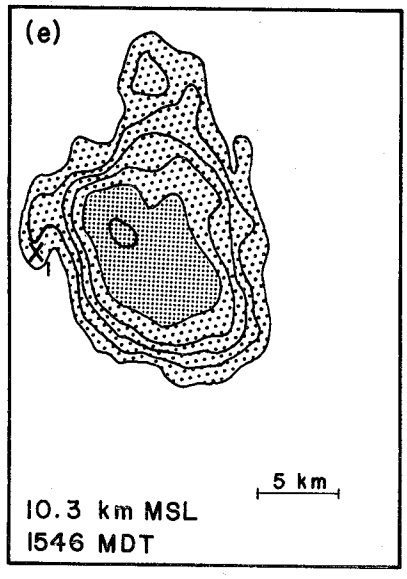
(e)
5 km
10.3 km MSL
1546 MDT

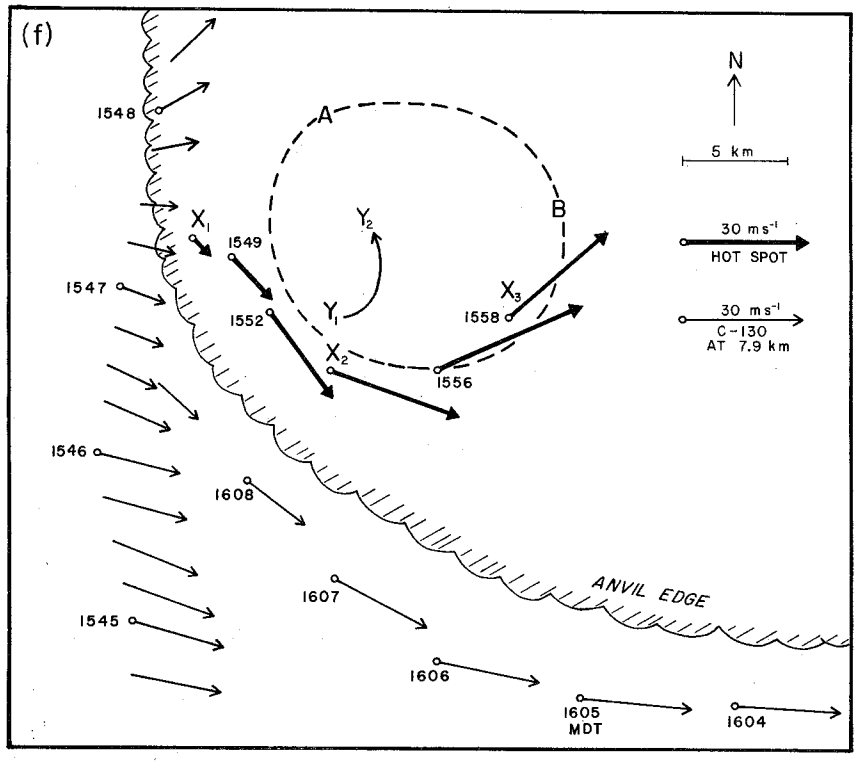
(f)
N
5 km
30 ms⁻¹
HOT SPOT
30 ms⁻¹
C-130
AT 7.9 km
A
B
X1
Y2
Y1
X2
X3
1548
1549
1547
1552
1546
1608
1607
1545
1606
1556
1558
1605
MDT
1604
ANVIL EDGE

Fig. 16 (cont.)

on the western (right) flank of the storm at X_1. Figure 16e shows that it appeared as a minor westward protrustion from the main echo. Many other hot spots formed in this same region, which we shall therefore refer to as the main embryo source region. Subsequently Hot Spot X traveled cyclonically around the embryo curtain, the level at which it was most clearly identifiable lowering toward the bottom of the embryo curtain by the time it had reached the southern flank. Until this time it had remained outside the mean position of the axis of maximum reflectivity but thereafter, as it approached the eastern flank, it crossed to the inside of the embryo curtain and began rising again as the particles encountered the more intense updrafts within the vault. Figure 16d shows the hot spot encroaching on the eastern part of the vault as it reached position X_3. At the same time that Hot Spot X began traveling around the embryo curtain, another echo hot spot, which originated a little closer to the axis of the embryo curtain, was tracked moving northward on the western boundary of the vault. Part of its track is depicted in Fig. 16f by Y_1Y_2. It appeared to be traveling at about 30 m s^{-1} but was not sufficiently well defined to enable a precise estimate to be made. Later figures (e.g., Fig 20b) are drawn to be consistent with both trajectories Y_1Y_2 and $X_1X_2X_3$. In the remainder of this section we shall restrict our attention to an analysis of the better defined Hot Spot X.

The velocity vectors plotted along the hot spot track $X_1X_2X_3$ in Fig. 16f show that the motion of the precipitation in the embryo curtain relative to the storm was initially rather slow on the western flank; however, it soon began to speed up and for most of the time it traveled along the axis of the embryo curtain at a velocity in excess of 30 m s^{-1} relative to the storm. Winds

measured by the C-130 just outside the cloud are also shown in Fig. 16f for part of a circumnavigation made close to this time period (this circuit was flown before that shown in Fig. 10). The two sets of data lead to a consistent picture of the flow field, including weak winds near an inferred stagnation point, as sketched in Fig. 10, and stronger winds along the southern flank of the storm both in the near environment and in the embryo curtain as air was diverted around the main updraft in the vault. Doppler radar measurements in another supercell storm (Brown, et al, 1973) have also shown the echo bordering the vault on its right flank to be associated with strong flow around the storm.

We are thus led to the three-dimensional flow pattern shown schematically in Fig. 17. According to this view, the updraft, with its strong southerly momentum, acted as an obstacle to the ambient westerly winds, producing aloft a common stagnation point which divided both flows into two branches. By eroding the updraft along its western boundary, the environmental flow probably forced part of the updraft air to circulate around the southern branch where particles embedded in the flow produced the embryo curtain. It is likely that most of the updraft followed a less deviated path and streamed around to the north and that both updraft flows eventually left the storm toward the east as together they formed the massive anvil outflow. Actually the two flows would have formed part of a single connected flow, the air between them (not shown in Fig. 17) having left the summit of the updraft directly toward the east.

Since the embryo curtain was located on the edge of the main updraft in the vault, any substantial mixing between the main updraft and air surrounding it would have brought particles from the embryo curtain into the vault. Since

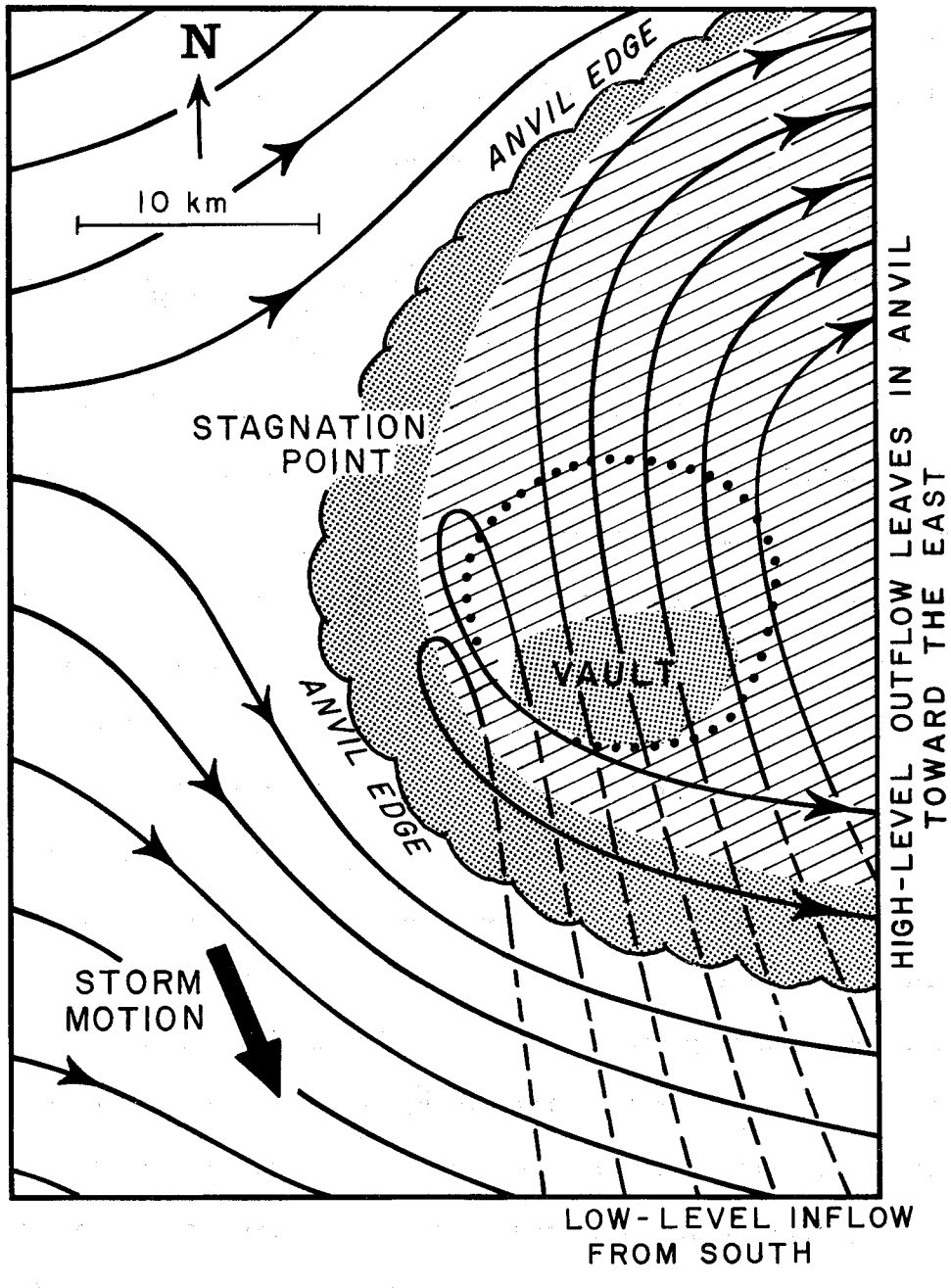

Fig. 17 Plan view showing schematically the principal features of the airflow within and around the Fleming storm at a time corresponding to the vertical section in Fig. 11. Regions of radar echo are shown hatched. Areas of cloud devoid of detectable echo are stippled. The dotted circle represents the extent of intense updraft in the middle troposphere. The thin lines are streamlines of airflow relative to the storm. Some of the streamlines represent environmental flow at middle-levels diverted around the main updraft. Others represent the low-level inflow toward the updraft (dashed lines) and also the high-level outflow.

this was not observed, we may conclude that the vault was essentially undiluted and contained close to an adiabatic concentration of water substance. This view is supported by measurements of adiabatic temperatures within the updrafts of severe storms by Davies-Jones (1974). Measurements by Grandia and Marwitz (1975) have indicated sub-adiabatic temperatures and liquid-water contents; however, their measurements were made in unbounded weak-echo regions of storms smaller than the present one in which greater mixing is likely to have occurred.

Although the embryo curtain was primarily influenced by the environmental flow, the fact that it was within cumuliform cloud and the fact that the C-130 experienced weak updrafts just outside the cloud suggest that it was itself within a transitional region of relatively weak updrafts. Probably these weak updrafts were fed from the shelf cloud (see Fig. 11). Because of the strong mixing with the dry environmental air implied by its circulation around the southern flank in the same manner as the environmental flow, the embryo curtain, unlike the main updraft, probably contained cloud water contents which were significantly sub-adiabatic.

An internal flow pattern similar to that in Fig. 17 was inferred for severe tornadic storms by Browning (1964), but the predominant stream of updraft air around the summit was considered to be the southerly flow rather than the northerly flow as in this case. That led to more and larger particles getting carried around in the southerly flow and falling toward the ground to form a well-developed hook echo (in contrast to the weakly-developed hook echo in the present case). It is possible that the difference between these two storms was due to a differing amount of cyclonic rotation within the updraft air, or to a different relation between the directions of the inflow and the

upper level winds, either of which would affect the position of the stagnation point and hence determine the proportion of updraft air diverted along the southerly route.

(b) Determination of the nature of the precipitation and vertical air motion around the embryo curtain

The inner edge of the embryo curtain marked the position where the updraft became strong enough to carry any re-entering embryos upward. Likewise the lower tip of the embryo curtain was the region where precipitation particles were re-entering the foot of the updraft, i.e., where the inflow was beginning to turn strongly upward to become the main updraft, as shown in Fig. 11. Figure 18a is a vertical section at 1554 showing the reflectivity distributions along the curved axis of the embryo curtain (cyclonically from A to B in Fig. 16f); it shows that precipitation was reaching the ground near A and B but that elsewhere the embryo curtain was forming a bridge over the inflow. The base of the embryo curtain was quite close to the 0C level, as shown in Figs. 11 and 18.

The vertical structure of Hot Spot X at a particular instant can be seen in Fig. 18a. The evolution of its vertical structure as it traveled around the embryo curtain is shown in the time-height section in Fig. 18b. In effect, this can be visualized as though it were a spatial cross-section along the track $X_1X_2X_3$ in Fig. 16f. Figure 18b shows that the region of locally more intense precipitation corresponding to the hot spot maintained a fairly constant altitude as it traveled around the embryo curtain (apart from a short-term fluctuation at 1548 which may have been due to difficulty in keeping track of the same hot spot at this time). This behavior can be used to infer the vertical air velocity in the region of the embryo curtain, but first we need to estimate the mean terminal fallspeed of the particles.

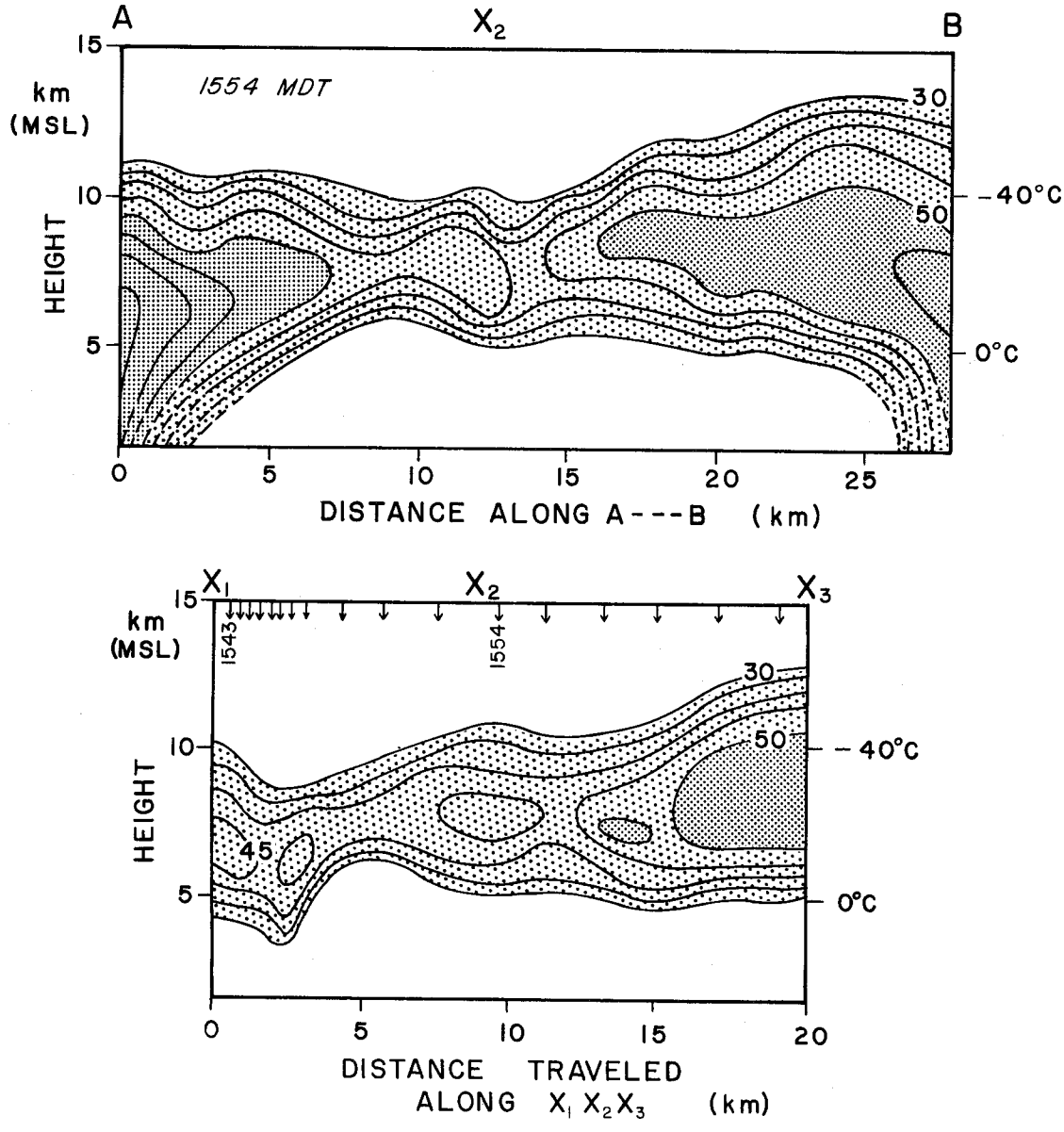

Fig. 18(a) Reflectivity distribution in a vertical section around the curved axis of the embryo curtain in the Fleming storm, cyclonically from A to B in Fig. 16(f).

Fig. 18(b) Reflectivity distribution in a time-height section through Hot Spot X as it traveled around the embryo curtain along the track $X_1X_2X_3$ in Fig. 16(f). The time scale has been plotted non-linearly to correspond to a linear distance scale as indicated at the foot of the diagram. Locations of the successive 1-min radar observations are indicated by arrows at the top of the diagram.

The maximum reflectivity of Hot Spot X was typically 40 to 45 dBZ. According to the relationship derived by Joss and Waldvogel (1970), this would imply a mean terminal fallspeed of about 10 m s^{-1} at the observed altitude if the particles were raindrops. The chances are, however, that the particles in the embryo curtain were mainly graupel particles and we shall compute their size from the equation $Z = 0.21\delta^2 ND^6$ (Atlas, 1964), assuming a monodisperse spectrum. Taking a reasonable concentration, N, of 1 to 10 m^{-3} (Musil, et al, 1975) and a mean density, δ, of 0.6 g cm^{-3}, the observed reflectivity corresponds to a diameter of about 6 mm. Such particles would also have a terminal fallspeed of about 10 m s^{-1}. The behavior of Hot Spot X is therefore consistent with such particles being balanced by a 10 m s^{-1} updraft. Of course, this is only intended to be a broadly representative value; superimposed on it there will have been a horizontal gradient of updraft velocity normal to the axis of the embryo curtain such that particles on the extreme inner edge of the embryo curtain are everywhere likely to have been rising on the edge of the vault as indicated in Fig. 11.

We have arrived at a picture in which the embryo curtain is seen to have been due to particles several millimeters in diameter within relatively weak and diluted updrafts traveling about the perimeter of the main updraft with a velocity comparable with that of the environmental air around the storm. The embryo curtain is likely to be a very important region as far as hail growth is concerned and it is a region where in situ measurements are greatly needed. Probably the most relevant observations to date are those of Marwitz (1972c) and Musil, et al (1973). According to Marwitz, an aircraft flying near cloud base penetrated "bullet-shaped echoes," corresponding to echo hot spots

in the embryo curtain. It encountered updrafts of about 5 m s^{-1} with hail of 1 to 2 cm diameter but no rain. Further analysis of data reported by Musil, et al (1973), has shown that pea-sized hail occurred in a region of a supercell storm corresponding to the embryo curtain; Sand (1974) reported a tendency for the hail in any given place to be monodispersed on that occasion. The little data that exists therefore suggests that the particles in the embryo curtain are more likely to be small hailstones or graupel rather than rain. This is also consistent with observations of Dye, et al (1974), that the ice crystal-graupel process is the dominant precipitation mechanism. In some circumstances, however--for example when the embryo curtain extends significantly below the 0C level--it may be characterized by rain as well as by hail. Haman (1967) and Morgan (1972) have shown that in this event the form of the airflow as sketched in Fig. 11 would imply the possibility for an accumulation zone of liquid water to develop within the embryo curtain.

9. The growth of hail in supercell storms

The foregoing analysis leads us to envision a three-stage process of hail growth, depicted schematically by Trajectories 1, 2 and 3 in Figs. 19a-b. Small particles are grown in the first ascent in the updraft (Trajectory 1). Some of these travel within weak updrafts around the perimeter of the main updraft (Trajectory 2) before re-entering the main updraft as embryos with a diameter of several millimeters. These recycled embryos then grow into hailstones during a simple up-and-down trajectory (Trajectory 3). We now consider the three stages of growth in turn:

Stage 1: Initial growth of the embryos during their first ascent in the updraft.

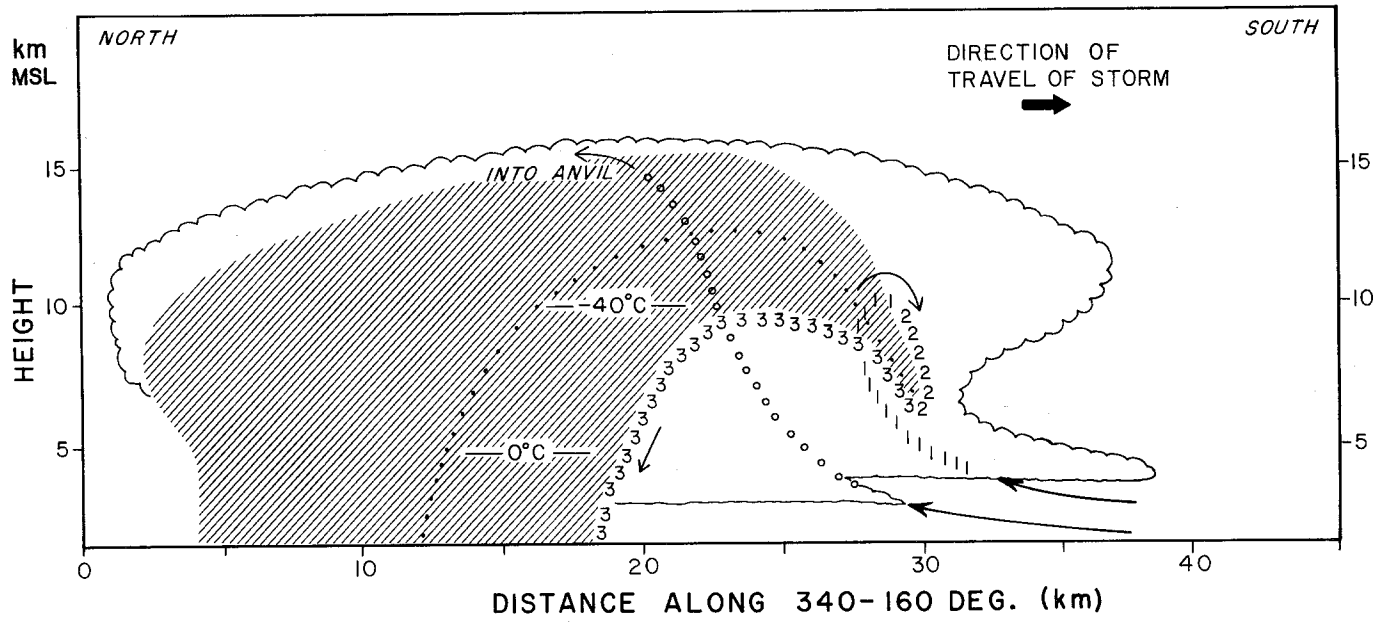

Fig. 19(a and b) Schematic model of hailstone trajectories within a supercell storm based upon the airflow model in Fig. 11. Fig. 19(a) shows hail trajectories in a vertical section along the direction of travel of the storm. Fig. 19(b) shows these same trajectories in plan view. The distribution of echo and cloud boundaries are as indicated in the airflow model in Figs. 11 and 17. Trajectories 1, 2 and 3 represent the three stages in the growth of large hailstones discussed in the text. The transition from Stage 2 to 3 corresponds to the re-entry of a hailstone embryo into the main updraft prior to a final up-and-down trajectory during which the hailstone may grow large, especially if it grows close to the boundary of the vault. Other slightly less favored hailstones will grow a little farther away from the edge of the vault and will follow trajectories resembling the dotted trajectory. Cloud particles growing "from scratch" within the updraft core are carried rapidly up and out into the anvil along Trajectory "0" before they can attain precipitation size.

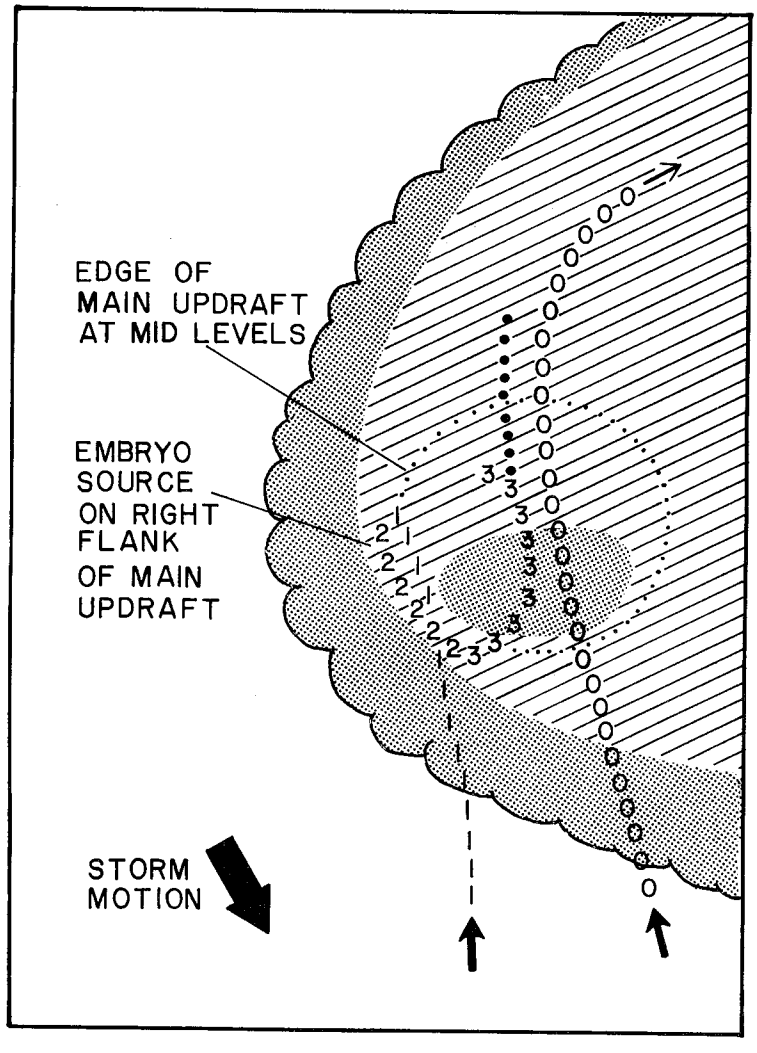
EDGE OF
MAIN UPDRAFT
AT MID LEVELS
EMBRYO
SOURCE
ON RIGHT
FLANK
OF MAIN
UPDRAFT
STORM
MOTION

Fig. 19(b)

There is evidence to suggest that in multicell storms there are usually secondary updrafts associated with cumulus congestus clouds on the flanks of the most intense updraft which successively intensify and take over the role of the main updraft (Dennis et al, 1970; Summers et al, 1972). Hailstone embryos are probably grown during the developing stage of these so-called feeder clouds and the embryos grow into hailstones as the feeder clouds become the main updraft. However, as in the case of the supercell storm reported by Marwitz and Berry (1971), major discrete feeder clouds do not seem to have existed in the Fleming storm. Thus we visualize the Stage 1 hail growth as consisting of small cloud particles growing "from scratch" within some part of the main updraft after initial condensation at cloud base. These small particles follow the airflow closely and ascend along the streamlines in and near the vault at typically 10 to 30 m s^{-1}, depending on whether they are on the edge or in the core of the updraft. Those in the core of the updraft ascend from cloud base to the -40C level in as little as 5 min after which they can grow no further because of total glaciation. The amount of growth in the absence of artificial seeding depends among other things on the availability of large condensation nuclei and efficient ice nuclei which might, for example, result from wind-raised soil particles (Rosinski et al, 1973); however, few particles are likely to grow larger than a few hundred microns during their ascent. As a result they are unlikely to attain a terminal fallspeed large enough for them to sediment, and aside from those that are accreted by hailstones growing above the vault, they will be carried along by the stream of air exhausting into the anvil outflow. These particles, denoted by Trajectory 0 in Fig. 19, are therefore lost to the hail process. On the other hand, particles growing in the relatively narrow region on the

edge of the updraft where the updraft speed is only about 10 m s^{-1} not only have more time to grow to millimeter size during their ascent, but also, stand a good chance of finding their way into the embryo curtain if they are grown on the western (right) flank of the updraft. These particles, growing from scratch on the western flank of the main updraft, are denoted by Trajectory 1 in Fig. 19.

Stage 2: Transfer of embryos from their growth region to the foot of the main updraft

Most of the small particles grown during the first ascent in the main updraft are carried away in the northerly branch of the outflow aloft (Fig. 17) and either evaporate or fall out in a location where they cannot re-enter the foot of the updraft. However, some particles are carried around in the southerly branch beneath the western edge of the updraft summit. Those which are large enough will fall into the region of weak updrafts that characterizes the embryo curtain. Some particles may also find their way from the main updraft into the embryo curtain by remaining within elements of the main updraft that are eroded away on its western flank as described in Section 8. These are represented by Trajectory 2 in Fig. 19. An unknown amount of further growth will occur within the weak updrafts characterizing the embryo curtain. Growth may be rather slow there since the liquid water is probably low. Some of the largest particles within the embryo curtain will fall to the lower tip of the curtain where they will re-enter the foot of the main updraft. They will then begin growing faster in the presence of more nearly adiabatic water contents. This picture provides the physical basis for the injection of embryos at the foot of a sloping updraft as postulated in hailgrowth models such as those of Browning (1963) and English (1973).

Stage 3: Growth of hail from embryos re-entering at the foot of the main updraft

This stage represents the growth of hail from embryos several millimeters in diameter during a single up-and-down cycle, as envisioned by Browning and English. A simple up-and-down trajectory of this kind would be consistent with the results of deuterium analyses by Knight, et al (1975); however, according to Macklin, et al (1970), deuterium analyses sometimes suggest further recycling of the growing hailstones.

Not all of the embryos re-entering the main updraft can be expected to grow into large hailstones; many may quickly encounter intense updrafts and be carried above the -40C level before they have had time to grow significantly. This is particularly likely if the updraft increases rather abruptly near the inner edge of the embryo curtain. According to Browning, et al (1963), it is the stringency of the requirement for the terminal fallspeed of these embryos approximately to match the updraft velocity, rather than an overall scarcity of embryos, which accounts for the paucity of large hail. Since the updraft speed in its core probably increases with height, those embryos re-entering the main updraft at the low levels, corresponding in this case to the tip of the embryo curtain, are likely to have the best chance of their terminal fallspeed being matched closely to the updraft velocity. These will stay longest in the growth region and will penetrate farthest into the updraft core. Having done so, these embryos will continue growing faster than any others by virtue of their exposure to adiabatic water contents, a favorable situation not enjoyed by smaller embryos rising faster above them which will encounter water contents already depleted by growth of the larger embryos. As a result of their rapid growth, the larger particles will tend to remain on the inner

(i.e., lower) edge of the embryo curtain and their trajectories will be limiting trajectories constituting the vault boundary, as shown by Trajectory 3 in Fig. 19a. These particles will reach their balance level at the top of the vault where, according to Atlas (1966), they will put on their major increment of growth before descending relative to the ground while all the time traveling with a component toward the north in the tilted updraft. They will then fall along the northern boundary of the vault where they will continue to be exposed to nearly adiabatic water contents as they approach the ground in the hail cascade.

The less favored embryos finding themselves in air depleted of some of its cloud water will grow into hailstones while following trajectories farther from the vault edge, as shown by the dotted trajectory in Fig. 19. According to List, Charlton and Buttels (1968), particles initially 5 mm in diameter being lifted through 2 km by a 24 m s^{-1} updraft would deplete the cloud water by only 3% or 20% according to whether their initial concentration was 1 or 10 m^{-3}, respectively. Thus the rate of growth of hailstones following trajectories such as the dotted one in Fig. 19 is unlikely to be diminished substantially by depletion provided the trajectories are not more than about 2 km above the inner edge of the embryo curtain (as measured along appropriate airflow streamlines). The fractional rate of depletion per unit height interval along a streamline is given by $\pi D^2 N V_t / w$, where D, N and V_t are the diameter, concentration and terminal fallspeed of the hailstones and w is the updraft velocity. Therefore, largely because of the increasing hailstone size, the depletion may become more severe as the stones rise over the vault apex. As discussed in the next section, however, the low precipitation efficiency of most supercell storms suggests that the overall depletion is rather small.

An important feature of the Stage 3 growth is that, although the air has a component of motion normal to the ceiling of the vault, the trajectories of the growing hailstones during this stage are roughly parallel to the edge of the vault. Thus the reflectivity of the echo bordering the vault increases from south to north along the hailstone trajectories (see the dashed curve above the vault in Fig. 7). The gradient of reflectivity normal to the edge of the vault is largely dictated by the radar resolution and is in no way a measure of the rate of growth. This is a different interpretation from that adopted by Young and Atlas (1974) in which the hailstones are assumed to increase in reflectivity while following trajectories almost normal to the ceiling of the vault.

The fact that the largest hailstones grow at the boundaries of the vault implies that they are growing not only in the presence of undepleted concentrations of small cloud droplets but also in the absence of accumulations of raindrops of the kind implied by the Soviet "rain storage" model (Sulakvelidze, et al, 1967). This was stressed by Browning (1967), who also pointed out that this kind of growth environment is consistent with the observations that large hailstones usually have a lobed structure and often contain relatively little unfrozen water.

Trajectory 3, when seen in plan view as shown in Fig. 19b, curves cyclonically as it leaves the region of the embryo curtain and travels over the vault. This curvature has been inferred from the shape of the region of higher reflectivity and from hot-spot trajectories such as Y_1Y_2 discussed in Sec. 8. The initial change from a west-east to a south-north direction is associated with the hailstones traveling from regions on the edge of the updraft, which are

strongly influenced by the environmental flow, toward the core of the updraft, in which there is a predominantly southerly flow. The final turn of Trajectory 3 toward the west as it travels to the north of the vault is associated with the stones falling from the updraft into the easterly winds characterizing the downdraft on the northern flank of the storm. This is consistent with the slope of the visual hailshaft depicted in Fig. 3.

We have chosen to refer to the hailgrowth as a 3-stage process; it might, however, be more appropriate to refer to it as a 2-stage process. This is because, depending on how close the Stage 1 trajectory is to the western edge of the main updraft, it might be possible to regard Stages 1 and 2 as occurring in the same kind of environment. There can, however, be no question of the reality of the major growth transition associated with the injection of Stage 2 embryos into the foot of the main updraft before the main Stage 3 period of hail growth.

This kind of model with recycling embryos implies that a hailstone embryo should exist as a distinct entity rather than as an arbitrarily-defined early stage in the growth of a hailstone. Observations of hailstones show that this is the case for large hailstones. According to Carte and Kidder (1966, 1970) and Knight and Knight (1970), virtually all stones with diameter larger than 2.5 cm exhibit distinct embryos several millimeters in size. Embryos are found to be distinct from the other parts of the hailstones in regard to other features, too, such as aerosol content for example. According to J. Rosinski (private communication), the aerosol particles in the embryos of large hailstones are usually small (less than 20 μm), whereas in the rest of the stone they tend to be large (up to 60 μm). This is consistent with most of the embryo growth

having taken place in a distinctly different region to that of the rest of the stone. It is also consistent with the embryo having grown within air originating far above the ground (Fig. 19a), while the rest of the stone is grown in air which has originated close to the ground and has been contaminated to a greater extent by wind-raised dust, especially just ahead of the storm's gust front. Long plumes of dust were indeed observed beneath the base of the updraft in the present case study (Fig. 13).

The lower tip of the embryo curtain was close to the 0C level in this study. Thus a small number of the embryos may have melted before re-entering the main updraft. This is consistent with the finding of Knight and Knight (1975) that, whereas small hailstones generally have graupel embryos, larger hailstones (more likely to have been grown in supercell-type storms) tend to have a mixture of graupel and frozen-drop embryos. As the Knights point out, it is difficult to explain the occurrence of different embryo types within the same sample of hailstones. One way would be to invoke a recycling mechanism of the kind described here.

An important study for the future is the collection and analysis of hailstones obtained from a supercell storm whose structure has simultaneously been observed by radar in the kind of detail discussed here. Both kinds of data provide insight into the nature of the hailstones' growth histories, and while neither data source alone allows a totally unambiguous interpretation, together they should limit the range of possible interpretations--especially if the hailstones are deep-frozen on collection and subjected to many different forms of analysis.

10. Evidence for inefficiency in the production of hail in supercell storms

The precipitation efficiency of some hailstorms tends to be low compared

with that of thunderstorms which produce rain only (Auer and Marwitz, 1968; Marwitz, 1972d). Supercell storms in particular have very low efficiency (Foote and Fankhauser, 1973). This is partly due to the combination of strong wind shear and dry environmental air which causes much of the precipitation to fall outside the updraft and evaporate. However, another reason for inefficiency in the production of precipitation is suggested by the large size of the vault in many supercell storms. The very existence of a vault implies inefficiency in conversion of cloud water to precipitation. Hail growing on the border of the vault accretes some of the supercooled cloud droplets and thereby converts some cloud water to precipitation. But when the ceiling of the vault is close to the -40C level, as in the present study, the cloud water rising within that part of the vault freezes homogeneously before it has been converted to precipitation. In this way a significant proportion of the cloud water in the updraft is able to pass through the entire storm system without ever being converted to precipitation. It is not just a matter of inefficiency in the production of rain; the failure of hailstone embryos to penetrate the vault also implies that the production of hail is not proceeding as efficiently as it otherwise could. The supercell is not, as Hitschfeld (1974) put it, "a closed system producing hail at a near capacity rate."

An extreme example of this kind of inefficiency has been illustrated by Marwitz (1972c). He describes a case in which the vault extended to the top of the storm. In that situation hailstones presumably did not penetrate far enough into the updraft core to be carried across it as in Trajectory 3 in Fig. 19. Many of the hailstones may simply have recirculated within the embryo curtain while traveling around the flank of the updraft and eventually

may have fallen to the ground ahead of the storm as hail of only moderate size. Although in the present study the evidence for inefficiency in hail growth was less dramatic, nevertheless there was indirect evidence that embryos were unable to penetrate into parts of the updraft core sufficiently far below the -40C level to achieve maximum growth. The evidence for this is the major indentation of echo between the two dashed axes of high reflectivity on the northern flank of the storm (Fig. 20a) which can be traced back up to the top of the storm just to the north of the vault apex. The two dashed axes on either side of the indentation represent vertically oriented sheets of hailstones descending within the predominantly northerly outflow from the updraft as sketched in Fig. 20b. Since the region of weaker echo between them was almost certainly within the same general outflow aloft, the weakness of the echo there must be attributed to the inability of large particles to be grown in the part of the updraft feeding this portion of the outflow. Such an idea is consistent with the fact that this part of the outflow passed close to the vault apex (VA in Fig. 20). Thus Fig. 20b (which is an elaboration of Fig. 19b drawn so as to take this added complexity into account) shows that large hail was able to grow along Trajectories 3 on either side of the vault apex presumably without rising far above the region of supercooled water. Particles following the path labeled XXX, however, experienced the strongest updrafts in the storm and, while being carried rapidly upward, passed over the vault apex into a region where they could no longer continue growing.

Inefficient though a supercell storm may be in converting cloud water to either rain or hail, paradoxically it is this very inefficiency that encourages the growth of large hail, provided that at least some embryos are able to re-

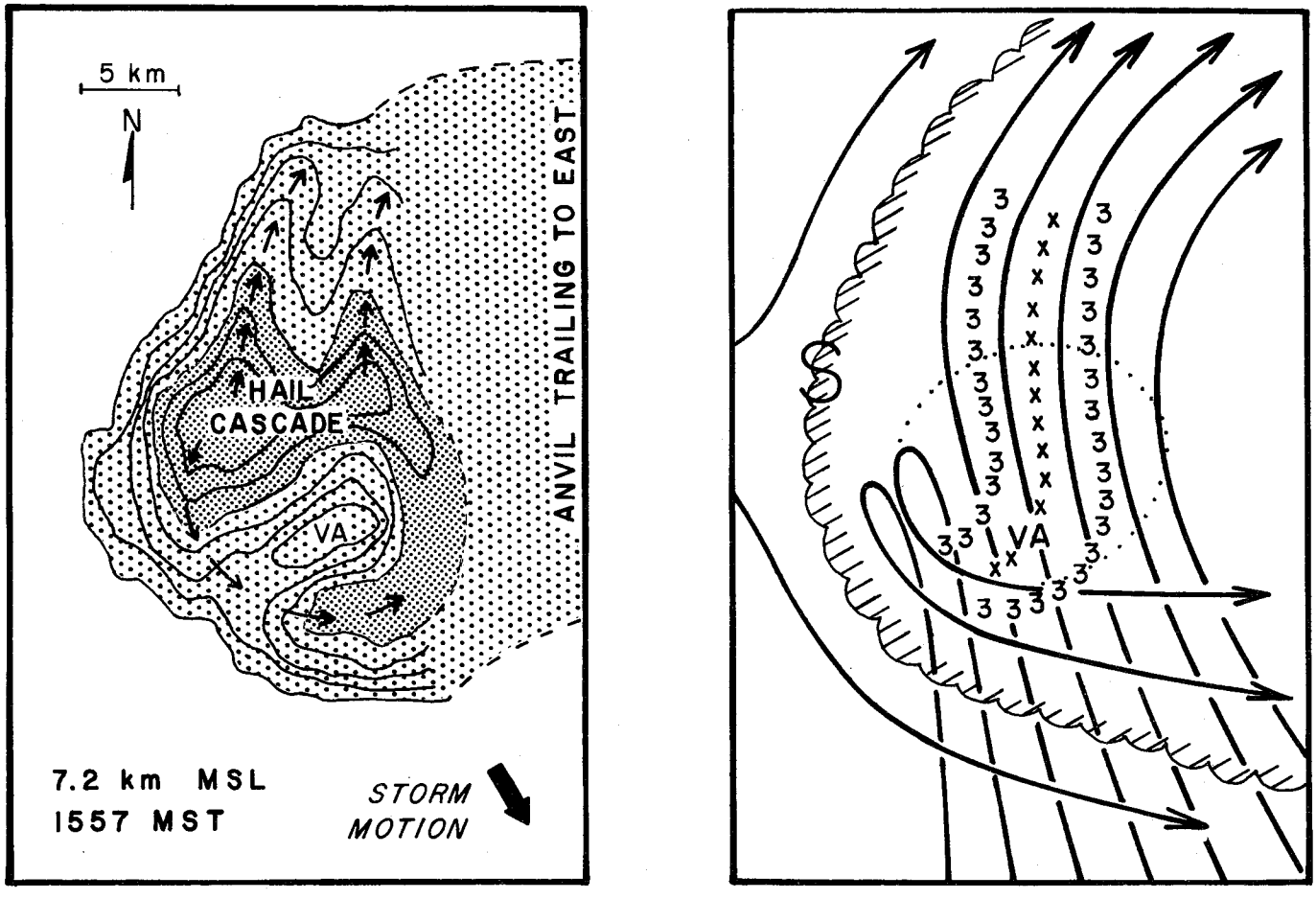

Fig. 20 Fig. 20(a) shows a quasi-horizontal section through the Fleming storm at 7.2 km MSL, showing reflectivity contours at 5 dB intervals above 30 dBZ. Arrows represent the motion of identifiable parts of the echo pattern. The indentation between the two northward-directed reflectivity maxima has considerable vertical extent and at higher levels can be traced back toward the vault apex (VA). Fig. 20(b) shows schematic streamlines of the airflow relative to the storm and also hail trajectories modified slightly from those in Fig. 19(b) so as to account for the echo indentation north of VA. As explained in the text, hail following either of the Trajectories 3 remained below the -40C level and continued to grow while crossing over the vault; hailstones following Trajectory XXX spent a lot of time above the -40C level and were not able to grow as large.

enter the main updraft. Without such inefficiency competition for the available cloud water would tend to limit the maximum hail size attainable.

11. Some implications for seeding supercell storms

We now investigate some of the implications of this model for hail suppression by silver iodide seeding. We shall consider three seeding approaches and, although we categorize them according to seeding location, it is important to note that they refer to three distinctly different seeding concepts.

(a) Seeding in or beneath the main updraft.

One approach to hail suppression is to generate additional embryos in the core of the main updraft in the hope of creating enough competition for the available water supply that no embryos grow into large hail. Our model suggests that there are major problems with this approach. As pointed out by Morgan (1972), any embryos developed as a result of seeding in the updraft core will ascend rapidly through the vault before they have grown big enough to be beneficial competitors. Most will leave the storm via the anvil outflow; however, a few may follow the path of some of the naturally generated embryos and find their way back into the embryo curtain as described in Section 9. Here they will indeed compete for the available cloud water; however, so long as the embryos do not grow so large as to be able to fall into the core of the vault and obliterate it, there will always be some particles near the edge of the vault that will compete unfairly by virtue of being the first to encounter the undepleted cloud water in the vault.

One factor that will tend to counteract the unfair competition is turbulence. This has the effect of interchanging particles on the edge of the vault with those suffering from depletion farther from the edge. The embryo curtain in the present study was viewed at a range as close as a few kilometers by the

the DC-6 airborne radar and the resulting high-resolution observations showed it to be a fairly smooth-edged feature with irregularities no larger than 500 m or so. This indicates that the outer scale to the turbulence was rather small and suggests that the turbulence may not have had a dominant effect in preventing unfair competition. Thus it seems that supercell storms exhibit a kind of natural selection mechanism which limits the number of embryos entering the hailgrowth region such that competition for the available water does not become an important factor Indeed as shown in Sec. 10, the natural selection mechanism may so restrict the entry of recycling embryos that the natural hail factory does not operate anywhere near its full capacity. These considerations may account for the apparent difficulties experienced by Soviet scientists in attempting to suppress hail in storms of the supercell variety (Marwitz, 1973b). Lack of apparent seeding effects has also been reported from experiments with a supercell storm in Alberta (Summers and Renick, 1971).

Browning (1965c) has presented an example of a possible natural hail suppression effect in supercell storms. He showed that several supercells in a family of storms produced widespread giant hail while they were developing the supercell structure but that in every case, although large hail continued to be produced, the size and extent of the hail diminished appreciably during the subsequent life of the supercells despite the storms remaining intense in other respects. We suspect that this apparent natural hail suppression effect was due to a shortage of suitable embryos re-entering the main updraft after it had become intense and well organized. If this is so in other supercells, then there is a danger that an increase in the concentration of embryos due to seeding might actually <u>increase</u> the amount of hail reaching the ground.

Consider the extreme example of the upper part of the vault extending through the -40C level. Here there is no depletion of the cloud water before it is lost to the hail process through natural glaciation. If seeding causes any embryos to find their way into the upper parts of such a vault, there can be no question that the tendency would be to generate more rather than less hail.

(b) Seeding the embryo source region on the storm's right flank.

So far we have only considered the possibility of competition for the available water during the growth of hailstones from embryos re-entering the main updraft. Another possibility is to promote competition during the growth of the embryos themselves by seeding the embryo source region on the right flank of the updraft. The objective here would be to decrease the size of the largest embryos circulating within the embryo curtain. We already know that the existence of the vault is due to the inability of embryos to attain sufficient size, and hence terminal fallspeed, to re-enter it and that as a result the hail production makes use of only a small proportion of the water supply (Sec. 10). If it were possible to decrease the terminal fallspeed of the embryos in the embryo curtain this should make the hail production even more inefficient by causing the embryos to be lifted more rapidly to the -40C level. They would then cross over the vault at levels where the updraft was glaciated naturally and in so-doing substantially decrease their time in the favorable growth region.

This seeding concept is in one sense the very opposite of the competing embryos concept. We are recognizing that there is a natural shortage of embryos in the main region of hailgrowth which is already making the hail process inefficient and we are trying to capitalize on this inefficiency by further decreasing the supply of embryos that are large enough to penetrate

the periphery of the main updraft. However, it is important to realize the limitations and dangers of this approach: first of all, we do not know the precise location of what we have called the "embryo source region." Second, if we were to seed at a rate inadequate to promote beneficial competition during the growth of the embryos, we would run the risk of generating additional embryos capable of entering the vault and producing more large hail as mentioned in Sec. 11(a).

(c) Seeding near the embryo curtain on the storm's front flank.

An alternative to generating competing embryos at one or another stage of their growth is to glaciate all or part of the updraft. The aircraft observations, analyzed in the manner described by Foote and Fankhauser (1973), show that the flux of water through the main updraft in the present case study was 10 kton s^{-1}. This is in line with the flux of water in other major supercell storms, although it is a factor of 2-10 larger than values determined by Auer and Marwitz (1968) for more typical hailstorms. Calculations by Young (1975) indicate that such a flux would imply the need to seed at a rate of 38 kg min^{-1} in order to glaciate effectively the entire updraft by the -26C level (i.e., reduce the liquid water to less than 5% of the total condensate), assuming that the mean updraft increased linearly from 10 to 40 m s^{-1} from cloud base to 10 km and that no natural ice multiplication occurred. Such a seeding rate would not be economically viable. Moreover, it would be logistically difficult to achieve a sufficiently widespread distribution of seeding material over the entire updraft. There is some reason to expect, however, that a useful effect might be achieved by seeding only the part of the updraft near the embryo curtain. The object would be to cause total glaciation locally so as to decrease the growth rate of the embryos in this region to the extent

that they would get carried to high levels before penetrating to the unseeded portions of the updraft by which time they would have risen above the -40C level. Although this approach would require only a small fraction (say 10%) of the seeding rate needed to glaciate the entire updraft, it may still be economically unattractive. In any case it would require very careful targeting of the seeding material and a good knowledge of the airflow.

Hosler (1974) has expressed concern about weather modification efforts in general in that, even if one is able to use a seeding technique to produce a desirable effect in one parameter, there is always the risk of simultaneously producing an undesirable effect in another. For example, seeding to suppress hail conceivably could lead to a decrease in rainfall. According to Borland and Snyder (1974), the beneficial effects of a 20% decrease in hail damage would be negated by a mere 5% decrease in total rainfall during the early growth season in northeast Colorado and Nebraska. However, while supercell storms may cause a significant proportion of hail damage, their rarity implies that they are responsible for a much smaller proportion of the season's rainfall. Thus, possible techniques for suppressing hail in supercells can be considered with rather less than the usual concern about the detrimental effects on rainfall.

12. Conclusions

Most attempts to suppress hail at present are based upon the idea that the growth of hail can be inhibited by creating many embryos that will compete for the available cloud water in the main updraft to the extent that none grows into large hail. Implicit in this competing embryo concept is the assumption that it is possible to introduce sufficient embryos into the main updraft. In the present paper we have presented evidence that this assumption is not valid

for what we have termed the archetypal supercell. The analysis in this paper has been based upon many detailed observations of just one storm; however, because of the well-defined nature of supercell storms, it is believed that this case study is representative of its class.

A characteristic feature of a supercell is its single intense quasi-steady updraft which propagates continuously without any other major distinct updraft nearby. A large part of the updraft core is characterized by inefficient conversion from cloud water to precipitation and is seen by radar as a weak echo vault. The growth of hail in a supercell has been discussed as a three-stage process. First: the growth of small embryos during initial ascent somewhere near the right (west) edge of the main updraft. Second: translation of some of these embryos from the upper levels within a sheathlike region of weak updrafts circulating around the forward (south) flank of the main updraft. Here the embryos give rise to a characteristically-shaped echo which we refer to as the embryo curtain. Third: particles from the embryo curtain re-enter the front of the main updraft and grow into large hailstones during a single up-and-down trajectory while skirting the upper boundary of the vault.

According to this three-stage growth model it appears difficult to introduce additional embryos into the main updraft to inhibit hail growth by the competing embryo concept. Any embryos developed as a result of seeding in the main updraft would ascend rapidly through the vault before they have grown big enough to be beneficial competitors. They would then either be carried out into the anvil outflow or would follow the paths of other naturally generated embryos and find their way back into the embryo curtain as described previously. Here they would indeed compete for the available cloud water; however, except in the unlikely event that the embryos grow large enough to

fall into the core of the vault and obliterate it, there will always be some particles near the edge of the vault that will compete unfairly by virtue of being the first to encounter the undepleted cloud water in the vault. In other words, a supercell storm exhibits a kind of natural selection mechanism which tends to restrict the number of embryos, natural or artificial, entering the hail growth region. As a result the "hail factory" does not work at anywhere near its full capacity and the production of additional embryos by seeding in the main updraft may increase the amount of hail rather than promote effective competition.

This does not preclude the possibility of suppressing hail on the basis of other concepts. For example, one way of suppressing hail in a supercell may be to recognize that the shortage of natural embryos entering the main updraft is already leading to inefficiency in the production of hail and hence to try to further decrease the number of large embryos in the embryo curtain. It is possible that this can be done by seeding the embryo source region on the storm's right flank so as to promote competition during the early growth of the embryos themselves. But first, however, we have to identify the location of the embryo source region more precisely than we have been able to in this study.

In this paper we have stressed steady state aspects of the organization of hailstorms. Most aircraft penetrations (e.g., Musil et al, 1975) and Doppler radar observations (e.g. Battan, 1975) of hailstorms reveal a greater degree of unsteadiness and non-uniformity in structure than we have shown here. This apparent contradiction is largely due to the fact that quasi-steady supercell storms have seldom been observed by the above techniques. But to some extent it is also due to our attempt to simplify the description of the physics of

the hailstorm by focusing on what we regard as the more essential features.

An important problem for the future will be to investigate the generality of the ideas developed here. Do they apply only to archetypal supercells, or do some of the ideas apply to other less well-organized storms as well?

Acknowledgments

The valuable assistance of C. G. Wade in various aspects of the analysis is greatly appreciated. We thank P. J. Eccles for obtaining and making available the fine 1-min scan sequences with the Grover radar. The contributions of J. C. Fankhauser, B. B. Phillips and H. Weickmann in collecting aircraft data and the support provided by the Research Aviation Facility, particularly the efforts of A. R. Rodi and T. H. McQuade, are appreciated. E. A. Mueller operated the CHILL radar system and kindly made the observations available to us. E. Ashworth ably performed the photogrammetric analysis. S. Borland provided the crop hail insurance figures. R. Vaughan and C. Mohr provided computer programming assistance. R. Coleman and C. Castillo drafted the figures. D. Atlas, Director of NHRE, made helpful comments on the manuscript.

References

Atlas, D., 1964: Advances in radar meteorology. Advances in Geophysics, 10, New York, Academic Press, 317-478.

_____, 1966: The balance level in convective storms. J. Atmos. Sci., 23, 635-651.

Auer, A. H., Jr. and J. D. Marwitz, 1968: Estimates of air and moisture flux into hailstorms on the High Plains. J. Appl. Meteor., 7, 196-198.

Barnes, S. L., 1974: Mesonetwork observations and analyses. NOAA Tech. Memo. ERL NSSL-69, 17-88.

Battan, L. J., 1975: Doppler radar observations of a hailstorm. J. Appl. Meteor., 14, 98-108.

Borland, S. W. and J. J. Snyder, 1974: Effects of weather variables on the prices of Great Plains cropland. Preprints, Fourth Conf. on Weather Modification, Ft. Lauderdale, Florida. Amer. Meteor. Soc., Boston, 545-550.

Brown, R. A., D. W. Burgess and K. C. Crawford, 1973: Twin tornado cyclones within a severe thunderstorm, single Doppler radar observations. Weatherwise, 26, 63-71.

Browning, K. A., 1962: Cellular structure of convective storms. Meteor. Mag., 91, 341-350.

_____, 1963: The growth of large hail within a steady updraught. Quart. J. Roy. Meteor. Soc., 89, 490-506.

_____, 1964: Airflow and precipitation trajectories within severe local storms which travel to the right of the winds. J. Atmos. Sci., 21, 634-639.

_____, 1965a: A family outbreak of severe local storms--a comprehensive study of the storms in Oklahoma on 26 May 1963. Air Force Cambridge Research Labs Special Report No. 32, 346 pp.

_____, 1965b: Some inferences about the updraft within a severe local storm. J. Atmos. Sci., 22, 669-677.

Browning, K. A., 1965c: The evolution of tornadic storms. J. Atmos. Sci., 22, 664-668.

_____, 1967: The growth environment of hailstones. Meteor. Mag., 96, 202-211.

_____, and R. J. Donaldson, Jr., 1963: Airflow and structure of a tornadic storm. J. Atmos. Sci., 20, 533-545.

_____, and F. H. Ludlam, 1962: Airflow in convective storms. Quart. J. Roy. Meteor. Soc., 88, 117-135.

_____, _____ and W. C. Macklin, 1963: The density and sturcture of hailstones. Quart. J. Roy. Meteor. Soc., 89, 75-84.

Byers, H. R. and R. R. Braham, 1949: The thunderstorm. Washington, D.C. U. S. Govt. Printing Office, 287 pp.

Carte, A. E. and R. E. Kidder, 1966: Transvaal hailstones. Quart. J. Roy. Meteor. Soc., 92, 382-391.

_____ and _____, 1970: Hailstones from the Pretoria-Witwatersrand area, 1959-1969. C.S.I.R. Res. Rept. 297, Pretoria, 1-42.

Chisholm, A. J., 1973: Alberta hailstorms, Part I: Radar case studies and airflow models. Meteor. Monograph, 14 (36), 1-36, Boston, Amer. Meteor. Soc.

_____ and J. H. Renick, 1972: "The kinematics of multicell and supercell Alberta hailstorms." Alberta Hail Studies 1972, Research Council of Alberta Hail Studies Report No. 72-2, pp 24-31.

Cunningham, R. M., 1960: Hailstorm structure viewed from 32,000 ft. Physics of Precipitation, Geophys. Monograph 5, Washington, D. C., Amer. Geophys. Union, 325-332.

Danielsen, E. F., R. Bleck and D. A. Morris, 1972: Hail growth by stochastic collection in a cumulus model. J. Atmos. Sci., 29, 135-155.

Davies-Jones, R. P., 1974: Discussion of measurements inside high speed thunderstorm updrafts. J. Appl. Meteor., 13, 710-717.

Dennis, A. S. and D. J. Musil, 1973: Calculations of hailstone growth and trajectories in a simple cloud model. J. Atmos. Sci., 30, 278-288.

_____, C. A. Schock and A. Koscielski, 1970: Characteristics of hailstorms of Western South Dakota. J. Appl. Meteor., 9, 127-135.

Dye, J. E., C. A. Knight, V. Toutenhoofd and T. W. Cannon, 1974: The mechanism of precipitation formation in northeastern Colorado cumulus. III. Coordinated microphysical and radar observations and summary. J. Atmos. Sci., 8, 2152-2159.

English, M. 1973: Alberta hailstorms, Part II: Growth of large hail in the storm. Meteor. Monograph, 14 (36), 37-98.

Fankhauser, J. C., 1971: Thunderstorm-environment interactions determined from aircraft and radar observations. Mon. Wea. Rev., 99, 171-192.

Foote, G. B. and J. C. Fankhauser, 1973: Airflow and moisture budget beneath a Northeast Colorado hailstorm. J. Appl. Meteor., 12, 1330-1353.

Fujita, T. and J. Arnold, 1963: Development of a cumulonimbus under the influence of strong vertical wind shear. Proc. Tenth Weather Conf., Amer. Meteor. Soc., Boston, 178-186.

Grandia, K. L., 1974: Aircraft observations within the weak echo region of High Plains thunderstorms. M.S. Thesis, U. of Wyoming, Dec. 1973, 92 pp.

_____ and J. D. Marwitz, 1975: Observational investigations of entrainment within the weak echo region. Mon. Wea. Rev., 103, 227-234.

Haman, K., 1967: On the accumulation of liquid water in a buoyant jet and its relation to hail phenomena. Acta Geophysica Polonica, 15, 9-27.

Hitschfeld, W. F., 1960: The motion and erosion of convective storms in severe vertical shear. J. Meteor., 17, 270-282.

_____, 1974: Hail suppression: evaluation and other problems. Preprints, Fourth Conf. on Weather Modification, Ft. Lauderdale, Florida, Amer. Meteor. Soc., Boston, 97-98.

Hosler, C. L., 1974: Overt weather modification. Reviews of Geophys. and Space Phys., 12, 523-527.

Joss, J. and A. Waldvogel, 1970: Raindrop size distributions and Doppler velocities. Preprints, Fourteenth Radar Meteor. Conf., 153-156, Boston, Amer. Meteor. Soc.

Knight, C. A., D. H. Ehhalt, N. Roper and N. C. Knight, 1975: Radial and tangential variation of deuterium in hailstones. Submitted to J. Atmos. Sci.

_____ and N. C. Knight, 1970: Hailstone embryos. J. Atmos. Sci., 27, 659-666.

_____ and _____, 1975: Hailstone embryo recirculation. Unpublished manuscript.

List, R., R. B. Charlton and P. I. Buttels, 1968: A numberical experiment on the growth and feedback mechanisms of hailstones in a one-dimensional steady-state cloud model. J. Atmos. Sci., 25, 1061-1074.

Lovell, C. C., 1974: The statistical design in the NHRE. Preprints, Fourth Conf. on Weather Modification, Ft. Lauderdale, Floriad, 99-102.

Ludlam, F. H., 1964: Final Report: Research on characteristics and effects of severe storms. Imperial College of Science and Technology, London. Air Force Cambridge Research Laboratories Contract No. AF 61(052)-254. May 1964, 12 pp.

Macklin, W. C., L. Merlivat and C. M. Stevenson, 1970: The analysis of a hailstone. Quart. J. Roy. Meteor. Soc., 96, 472-486.

Marwitz, J. D., 1972a: The structure and motion of severe hailstorms. Part I: Supercell storms. J. Appl. Meteor., 11, 166-179.

_____, 1972b: The structure and motion of severe hailstorms. Part II: Multicell storms. J. Appl. Meteor., 11, 180-188.

_____, 1972c: The structure and motion of severe hailstorms. Part III: Severely sheared storms. J. Appl. Meteor., 11, 189-201.

_____, 1972d: Precipitation efficiency of thunderstorms on the High Plains. J. Rech. Atmos., 6, 367-370.

_____, 1973a: Trajectories within the weak echo regions of hailstorms. J. Appl. Meteor., 12, 1174-1182.

_____, 1973b: Hailstorms and hail suppression techniques in the USSR - 1972. Bull. Amer. Meteor. Soc., 54, 317-325.

_____, A. H. Auer, and D. L. Veal, 1972: Locating the organized updraft on severe thunderstorms. J. Appl. Meteor., 11, 236-238.

_____ and E. X Berry, 1971: The airflow within the weak echo region of an Alberta hailstorm. J. Appl. Meteor., 10, 487-492.

Moncrieff, M. W. and J. S. A. Green, 1972: The propagation and transfer properties of steady convective overturning in shear. Quart. J. Roy. Meteor. Soc., 98, 336-352.

Morgan, G. M., Jr., 1972: On the growth of large hail. Mon. Wea. Rev., 100, 196-205.

Musil, D. J., E. L. May, P. L. Smith, Jr., W. R. Sand, 1975: Precipitation particle size observations inside Northeast Colorado hailstorms. To be submitted for publication.

_____, W. R. Sand and R. A. Schleusener, 1973: Analysis of data from T-28 aircraft penetrations of a Colorado hailstorm. J. Appl. Meteor., 12, 1364-1370.

Nelson, S. P. and R. R. Braham, 1972: Detailed observational study of an echo free region. Preprints, Fifteenth Radar Meteor. Conf., Champaign-Urbana, Ill., Amer. Meteor. Soc., Boston, 57-60.

Newton, C. W. and H. R. Newton, 1959: Dynamical interactions between large convective clouds and environment with vertical shear. J. Meteor., 16, 483-496.

Roach, W. T., 1967: On the nature of the summit areas of severe storms in Oklahoma. Quart. J. Roy. Meteor. Soc., 93, 318-336.

Rosinski, J., C. T. Nagamoto, T. C. Kerrigan, and G. Langer, 1973: Freezing nuclei derived from soil particles. J. Atmos. Sci., 30, 644-652.

Sand, W. R., 1974: Use of the armored T-28 aircraft to obtain observations in hailstorms with emphasis on the characteristics of the high radar reflectivity zones. Report 74-14, Institute of Atmos. Sci., South Dakota School of Mines and Tech., Rapid City, South Dakota, 76 pp.

Sulakvelidze, G. K., H. Sh. Bibilashvili and V. F. Lapcheva, 1967: Formation of precipitation and modification of hail processes. Translated by Israel Program for Scientific Translations, Jerusalem, 208 pp.

Summers, P. W., 1972: Project Hailstop: A review of accomplishments to date, in Alberta Hail Studies 1972. Research Council of Alberta, Hail Studies Report 72-2, pp. 47-53.

_____, G. K. Mather and D. S. Treddenick, 1972: The development and testing of an airborne droppable pyrotechnic flare system for seeding Alberta hailstorms. J. Appl. Meteor., 11, 695-703.

_____ and J. H. Renick, 1971: Case studies of the physical effects of seeding hailstorms in Alberta. Proceedings, International Conf. on Weather Modification, Canberra, Australia, Amer. Meteor. Soc., Boston, 213-218.

Young, K. C., 1975: Growth of the ice phase in strong cumulonimbus updrafts. To be submitted to Pure and Applied Geophysics.

_____ and D. Atlas, 1974: NHRE Microphysics: an overview with emphasis on hail growth and suppression. Preprints, Fourth Conference on Weather Modification, Ft. Lauderdale, Florida, Amer. Meteor. Soc., Boston, 119-124.